Assessing the feasibility and scalability of short-haul battery-electric aviation in Europe:

Coupling ML-based demand forecasting, network modelling and GHG mitigation potential under battery constraints

Thijs W. Savelberg*
MSc Aerospace Engineering
Delft University of Technology
Delft, Kluyverweg 1, 2629 HS

Netherlands Airport Consultants (NACO)
Delft, Mijnbouwstraat 120, 2628 RX

Abstract

Battery-electric aviation represents a promising pathway to substantially reduce the overall climate impact of short-haul air transport. This includes complete elimination of both in-flight CO_2 and non-CO_2 effects. Nevertheless, considerable debate and uncertainty remain regarding whether the technology can achieve meaningful scale and deliver a significant impact at continental level. Previous studies, however, have typically examined technical, economic, or environmental feasibility aspects in relative isolation, often focusing on specific routes or individual aircraft types. This thesis addresses these gaps through an integrated framework that couples machine-learning-based demand forecasting, algorithmic network design, uncertainty modelling, and sector-wide GHG mitigation assessment under realistic gravimetric battery energy density constraints. A custom Python-based software tool with an interactive Streamlit dashboard enables evaluation of any combination of European airports and announced electric aircraft types, as well as a fully customisable aircraft model for extensive sensitivity and scenario analysis.

Key results show that the XGBoost model predicts baseline demand on unserved routes with high accuracy ($R^2 = 0.79$, SMAPE = 18.7%). Electric aircraft could induce approximately 25.1% additional demand through reduced operating costs and higher willingness-to-pay for zero-emission flights. Under projected near- to mid-term solid-state battery pack energy densities (356–480 Wh/kg), 13.8–22.3% of European aviation sector CO_2 emissions could be avoided. Network design identifies an intra-European early-phase hub-and-spoke configuration requiring charging at only 15 strategic hubs plus two connectors, while maximising electrifiable passenger demand. The study shows that battery-electric aviation outperforms competing technologies on short-haul routes in terms of cost, emissions, and energy efficiency. However, achieving the full 22.3% decarbonisation potential requires electrifying more than 50% of all European flights, which translates into challenges, as the R&O analysis of this study shows. Collaborative action as well as incentives and targeted policy support will be essential and will require a shift from Europe's rather isolated focus on SAF. The network configurations presented in this study provide a strong starting point for collaborative development, while recommendations for future research include realistic decarbonisation pathways integrating the phase-out of conventional aircraft and the study of high-impact policy measures.

*This MSc thesis was completed at Delft University of Technology, Faculty of Aerospace Engineering, in collaboration with Netherlands Airport Consultants (NACO)

Supervisors: P.C. Roling, J. Ribeiro, P. Proesmans

Delft University of Technology (24-4-2026)

Nomenclature

GAIS	Geospatial Airport Information System	**SMAPE**	Symmetric Mean Absolute Percentage Error
PPDEW	Passengers Per Day Each Way	**XGBoost**	eXtreme Gradient Boosting
SHAP	SHapley Additive exPlanations	**TEN-T**	Trans-European Transport Network
TreeSHAP	Tree-specific implementation of SHAP	**PT**	Pass-through rate of cost savings to ticket price
WTP	Willingness To Pay	**R&O**	Risk and Opportunity
CAGR	Compound Annual Growth Rate	**I(s,T)**	Drive-time isochrone around airport s at time T
ERF	Electric Range Factor		
SSB	Solid-State Battery		
TRL	Technology Readiness Level	D_y	Projected annual demand in year y
SAF	Sustainable Aviation Fuels	$D_{\textbf{base}(y_0)}$	Baseline demand in reference year y_0
GHG	Greenhouse Gases	ε	Price elasticity of demand
CO_2	Carbon dioxide	ΔC	Operating cost reduction
Wh/kg	Watt-hour per kilogram (gravimetric energy density)	g	Compound annual growth rate
R^2	Coefficient of determination	ϕ_i	SHAP value (feature contribution)
MAPE	Mean Absolute Percentage Error		

1 Introduction

The aviation sector faces growing pressure to achieve net-zero greenhouse gas emissions by 2050. This pressure arises from the global commitments of the Paris Agreement [4] and is strengthened in Europe by the European Green Deal [2] and the Fit for 55 package [34]. Within this policy framework, ReFuelEU Aviation [83] serves as the main binding instrument specifically designed to increase the supply and uptake of sustainable aviation fuels (SAF). SAF are currently widely regarded as the most straightforward near-term solution for aviation decarbonisation [9, 13, 38]. These fuels offer full drop-in compatibility with existing aircraft and infrastructure, while providing life-cycle CO_2 emission reductions of up to 80%, depending on the used feedstock and production method [63].

Nevertheless, SAF production is still in its early stages. Large-scale deployment is hindered by limited sustainable feedstock availability, production costs that are typically three to five times higher than conventional jet fuel, and competition for renewable resources with other sectors [59, 64]. Current projections indicate that SAF alone will not be sufficient to meet aviation's decarbonisation targets [9, 17]. A diversified portfolio of technologies is therefore required. On short-haul routes, battery-electric propulsion is viewed as the most promising option, thanks to its superior energy efficiency, significant reductions in both CO_2 and non-CO_2 emissions, and favourable long-term cost potential [21, 30, 59, 78].

However, for many years, battery-electric aircraft were considered impractical for commercial operations at meaningful scales, mainly due to limitations in battery energy density [60]. Recent design innovations have started to change this view [29, 90]. A prominent example is the Elysian E9X, a 90-seat regional concept aiming for a range of 800 km using near-term battery technology [30, 59]. This is achieved through optimised aerodynamics, advanced battery integration, and improved overall energy efficiency [30]. These advances show that considerable ranges are achievable and that regional electric flight can provide pathways that even surpass alternatives in both efficiency and CO_2-eq climate impact reduction.

Despite these developments, existing research often focuses on isolated aspects, such as battery performance [71], techno-economic viability of selected routes [16], or specific emission profiles

[31]. This fragmented approach overlooks the important interactions between demand induction, network topology, infrastructure roll-out, battery constraints, and overall environmental benefits. These interactions are critical for determining real-world feasibility and scalability in the European context.

In addition to filling the key research gaps identified for each individual module (detailed below), this thesis addresses the 'interdependency gap' by adopting a coupled multi-module framework that explicitly models the interactions between the four components. This is done in collaboration with Netherlands Airport Consultants (NACO) as part of the TU Delft Aerospace Engineering master's programme. The work introduces a custom Python-based software tool with a Streamlit dashboard for visualisation and strategic planning. The tool enables evaluation of arbitrary combinations of EU airports and announced electric aircraft types. Unlike studies limited to specific cases, it is designed for general applicability and supports airport clients in infrastructure planning, demand forecasting, and decarbonisation strategy. The analysis is structured in four interconnected parts that each extend to specific research gaps that were identified within the literature study of this research:

- **Module 1: Machine-Learning Based Demand Forecasting Model and Electrification-Induced Traffic Assessment for unserved routes**

  Several studies suggest that lower operating costs of electric aircraft, driven by reduced energy and maintenance expenses, could generate potential induced demand [7, 40, 84]. However, this effect has rarely been quantified, particularly its potential to make previously unserved routes economically viable. Module 1 addresses this gap by developing a machine-learning-based demand forecasting model. The model first estimates baseline demand for unserved routes with an XGBoost decision tree network and then extends it with two induced demand components resulting from decreased operating costs and increased passengers' willingness to pay for sustainable transport. These are combined with appropriate compound annual growth rates (CAGR) to reflect evaluation of future years. The framework further incorporates Shapley Additive Explanations (SHAP) [35] for interpretability [55, 56] and accounts for broader market dynamics. Additionally, the 2040 European TEN-T high-speed rail network [10] is programmed into the software tool to provide alerts for competition and comparison of travel times. Sensitivity analyses across varying cost reductions, Willingness to Pay (WTP) parameters, demand elasticities, and projected annual growth rates provide a wide variety of novel insights into the induced demand achievable with electric aviation and its potential to connect smaller economies.

- **Module 2: Initial Deployment and Minimal-Infrastructure Hub-and-Spoke Network Modelling for served routes**

  Previous studies have often highlighted promising regions for early electric aircraft deployment, such as mountainous, water-surrounded, or remote areas [33, 57]. However, they rarely examine well-suited network structures for initial roll-out under realistic minimal infrastructure constraints. Module 2 addresses this gap by first generating hub-and-spoke networks that rely on semi-range flights operated from a limited number of strategically selected hubs. This structure helps overcome the chicken-and-egg problem by enabling coordinated deployment between airlines and airports in suitable, high demand regions. Three additional sub-tools then support network extension: they map electrifiable route segments, recommend suitable aircraft types for minimum frequency increase, and evaluate onward electrifiable connectivity. These complementary tools thereby assess point-to-point route viability for later deployment stages, gradually complementing the core network.

- **Module 3: R&O Assessment and Battery Technology Uncertainty Framework**

  Existing literature highlights a broad range of risks and opportunities related to battery technology for aviation, yet these factors are usually discussed in isolation and their relative importance remains difficult to compare [15, 48, 52]. The National Renewable Energy Laboratory (NREL) specifically recommends the dedicated development of global risk matrices as an extension to their research: "Overview of Potential Hazards in Electric Aircraft Charging Infrastructure [74]. Module 3 addresses this gap by developing global

risk and opportunity matrices that consolidate diverse risks and opportunities drawn from past experiments, earlier studies, and ongoing research projects. The matrices enable a structured comparison of impact and probability within a single framework. They are constructed twice for risks: once before and once after applying potential mitigation strategies identified in the literature. For opportunities, amplification strategies are applied to maximise potential benefits. In addition, a dedicated battery technology uncertainty tool translates different energy density scenarios into achievable range performance. These energy-density–range relations feed directly into the demand forecasting and network analyses of Modules 1 and 2, allowing route viability to be examined as a function of anticipated battery performance. The same relations also support the environmental impact assessment in Module 4. Conversely, the Geospatial Airport Information System (GAIS) developed for the other modules enables a joint large-scale averaging analysis across more than 800,000 scenarios, which in turn strengthens the conclusions drawn in Module 3.

- **Module 4: Environmental Impact Assessment and GHG Mitigation Potential**

  Although industry-wide emission reduction potentials of electric aviation have been assessed in earlier research, these studies rarely link the outcomes directly to battery energy density [59, 81]. Module 4 addresses this gap through a comprehensive environmental impact assessment. Using the battery technology uncertainty framework from Module 3, it calculates industry-wide CO_2 avoidance potential as a function of gravimetric energy density by integrating interpolated emission data across different range segments. This approach enables extensive scenario analysis and provides novel insights through the derivative of the resulting curves, which directly translate incremental improvements in battery energy density over the coming decade into potential decarbonisation gains. The module additionally visualises CO_2-eq emission impact using external data [59] and quantifies the enormous energy demand associated with e-fuel production. By comparing the renewable electricity demand required to produce e-fuels sufficient for KLM's annual operations to the Netherlands' total renewable electricity consumption, the analysis highlights the substantial energy-efficiency advantage of battery-electric aviation.

This thesis presents a compact summary of the methodology and main findings developed in the full research. As the present work is a scientific paper derived from a complete master's thesis, only the core elements of the framework and the most important results are discussed here. More detailed descriptions of the models, tools, assumptions, and extensive sensitivity analyses are provided in the full thesis report [76].

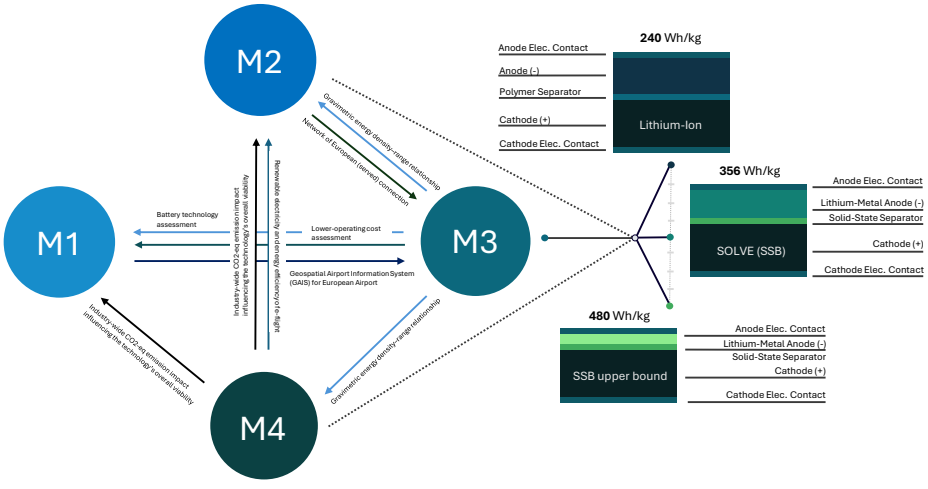

Figure 1: Inter-dependencies and over-coupling influence of gravimetric battery-pack energy density

2 Methodology

The methodology section comprises the four interdependent modules outlined in the introduction. Each module is implemented as a self-contained Python tool and linked through shared components, principally the developed Geospatial Airport Information System (GAIS) and the battery pack gravimetric energy density-range relation. The latter directly impacts all modules and propagates consistently through every analysis. This enables systematic evaluation of more than 800 000 different electrification scenarios while preserving uniformity of assumptions. Basic principles and high-level workflows are explained in the main text; detailed visualisations, underlying assumptions, mathematical derivations, and sensitivity analyses are provided in the appendices. These appendices form an integral part of the paper and are strongly recommended for a complete understanding of the developed tools and models.

2.1 Module 1: Machine-Learning Based Demand Forecasting Model and Electrification-Induced Traffic Assessment for unserved routes

To assess the deployment potential of battery-electric regional aircraft on currently unserved European routes, a dedicated demand forecasting tool was developed as an interactive Python-based dashboard. The tool combines aircraft performance constraints, route filtering, accessibility evaluation, catchment-area market estimation, machine-learning-based demand prediction, and induced-demand modelling into a unified workflow.

2.1.1 Tool Configuration and Development of Geospatial Airport Information System (GAIS)

An input menu, as shown in Appendix E, was designed that enables specification of an origin airport anywhere in Europe and selection of one of four battery-electric aircraft types under development and included in this study: Vaeridion Microliner [11], Eviation Alice [5], Heart Aerospace ES-30[2] [8], or the Elysian E9X [30]. This selection includes all non-hybrid all-electric aircraft with announced market entry in the coming decade and a minimum capacity of 9 passengers. Strictly speaking, the Elysian E9X is a hybrid configuration, however, as its turbo-generator serves as a backup energy system for loiter and diversion only [30], it is included as the only exemption. Each aircraft is parametrised by its operational range, passenger capacity, cruise speed, and minimum required runway length, as provided by the respective manufacturers [5, 8, 11, 30]. These parameters all play a role in the identification of viable destination airports.

In addition to the four listed aircraft types, a separate interface was designed that allows the definition of a hypothetical aircraft by manually entering its design parameters. This design option is directly coupled to the battery gravimetric energy density-range tool, designed in module 3 of the software application. This allows for extensive sensitivity analysis over a wide spectrum of potential battery development scenarios.

Airport data are obtained from the OurAirports database which provides coordinates, runway lengths, IATA/ICAO codes, and facility classifications [70]. These datasets were complemented with intra-European flight schedule data from SABRE [75] and NACO [61] as well as additional airport- and country specific parameters (language [39], gross domestic product (GDP) [46], and catchment population [37, 68]) all collected for the ML-model, as further detailed in subsection 2.1.3. The full integration of these datasets, connected to a visualisation package (Folium [41]) together create a 'Geospatial Airport Information System (GAIS) for European Airports'. This system will be referred to as 'GAIS' in the remainder of this report.

2.1.2 Route Viability Assessment and Accessibility Gain Study

For any given origin–aircraft combination, candidate destinations are identified by applying the haversine formula to compute great-circle distances and retaining only those within the aircraft's operational range. A subsequent filter excludes airports whose longest runway is shorter than the selected aircraft's minimum required runway length. Consequently, purely military airfields are

[2]Heart Aerospace has announced a phased ES-30 roadmap comprising an electric 200 km and hybrid 400 km variant (late 2020s), followed by electric 300 km / hybrid 500 km (mid-2030s) and electric 400 km / hybrid 600 km (late 2030s). This study uses the announced 400 km fully electric variant by default. The interactive software tool also includes a fully customisable aircraft model that allows evaluation of all announced variants.

removed (via type classification and keyword matching), and only locations with both valid IATA and ICAO codes are retained. The latter being a strong indicator of scheduled commercial passenger capability.

A reference network of existing scheduled services (derived from NACO data [61]) is used to classify the remaining connections as served and unserved. The example displayed by Figure 5a shows how these routes are marked navy blue and light blue, respectively. Routes located within 80 km straight line distance (≈60 min driving distance) of an already served airport are separately flagged (purple) to account for likely surface-access competition.

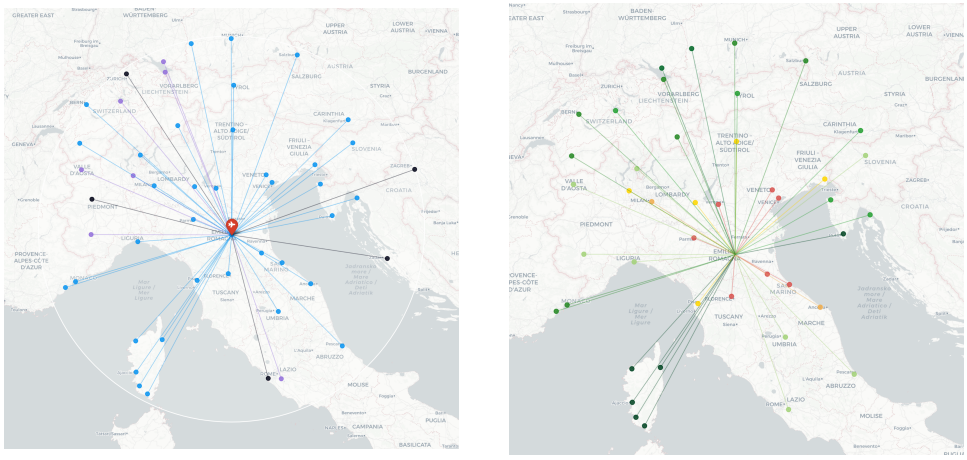

(a) Identification and categorization of viable destinations based on aircraft parameters and GAIS

(b) Accessibility gain study comparing travel times of electric aviation to car transport, using Open Street Maps (OSM)

Figure 2: Preliminary analysis of the deployment of the Heart Aeropsace ES-30 for Bologna Guglielmo Marconi Airport (BLQ)

To identify routes where electric aviation can offer substantial time advantages, an accessibility assessment is performed. For each potential destination, fastest road travel times are calculated using OpenStreetMap [69] data combined with a shortest path algorithm, integrating the maximum driving speed parameters of each road segment. Electric flight block time is estimated based on great-circle distance and the cruise speed of the electric aircraft. Furthermore, a fixed 45-minute allowance for airport procedures is added. The accessibility gain ratio (road time / electric flight time) is computed for each unserved connection and visualised with a colour scale, as shown by Figure 2b. Routes with road times below 2.5 hours are highlighted in red, regardless of the accessibility ratio, due to particularly strong ground-mode competition.

2.1.3 XGBoost Model Development, Training and Performance Evaluation

Routes identified as high-potential or any specific route of interest to the user of the tool, can be manually selected to initiate the detailed demand forecasting procedure. The demand forecasting process is based on several airport and route-specific variables that allow for estimation of the air-demand between two airports. One of the key variables is obtained by computing catchment areas delineated as 60-minute drive-time isochrones around each airport (computed via OpenRouteService [68]) and overlaid on 100 m gridded population data, from the Global Human Settlement Layer [37]. Example isochrones are visualised by Figure 3, whereas Appendix C provides more insights into the mathematical computations leading to these catchment areas and the population figures. The resulting origin and destination catchment populations of each potential route are combined with great-circle distance, country-level GDP per capita [46], domestic/international status, and a binary indicator of shared official language [39], potentially spoken in both the origin and destination countries of the evaluated route.

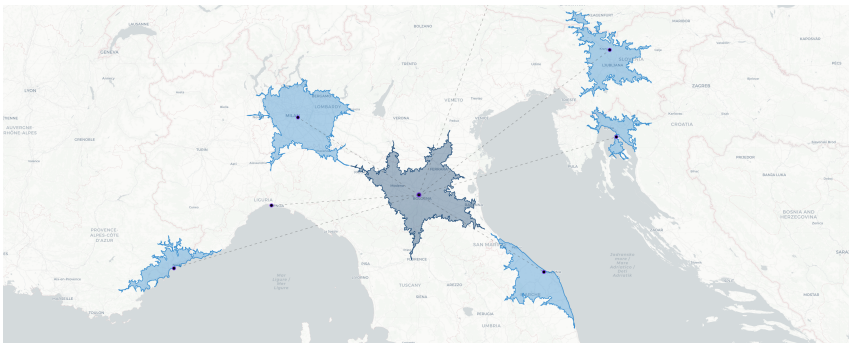

Figure 3: 60-minute isochrone catchment area analysis for potential routes from Bologna Guglielmo Marconi Airport (BLQ)

The demand forecasting model was trained on 2024 SABRE [75] intra-European route data (∼27 000 routes) of which the actual demand was known. Therefore, all the previously listed input variables of the model had to be collected for these routes to yield predictions and compare these to the actual demand figures. After exclusion of major hubs, extreme volume outliers, and very small catchments populations (<20 000), a conventional gravity model was initially designed and applied. However, this model achieved insufficient performance ($R^2 \sim 0.48$, MAPE $\sim 56\,\%$). Alternative approaches were therefore evaluated. These included a Convolutional Neural Network (CNN), Decision Tree, Random Forest and XGBoost (eXtreme Gradient Boosting) framework. After testing all models, XGBoost consistently demonstrated superior predictive accuracy. Therefore, XGBoost, visualised by Figure 4, was found to have the best capacity to model the non-linear interactions and heterogeneous route characteristics of European regional air transport, while incorporating effective regularisation.

The final model employs seven engineered features: natural logarithms of distance, origin–destination GDP-per-capita and catchment-population products and sums, plus binary indicators for domestic routes and shared official language. These variables were chosen as they have proven to capture solid predictive dynamics in earlier research [18, 27, 43, 91], and as they are computable for all $\sim$ 700 airports included in the analysis. This latter was an important criterion given the hard requirement of the tool to be applicable to any desired combination of European airports. Lastly, it is relevant to note that annual passenger volumes were subjected to Yeo–Johnson transformation prior to training to reduce skewness and stabilize variance [88]. Hyper-parameters were optimised using Bayesian optimisation [50] under 5-fold distance-stratified cross-validation [77].

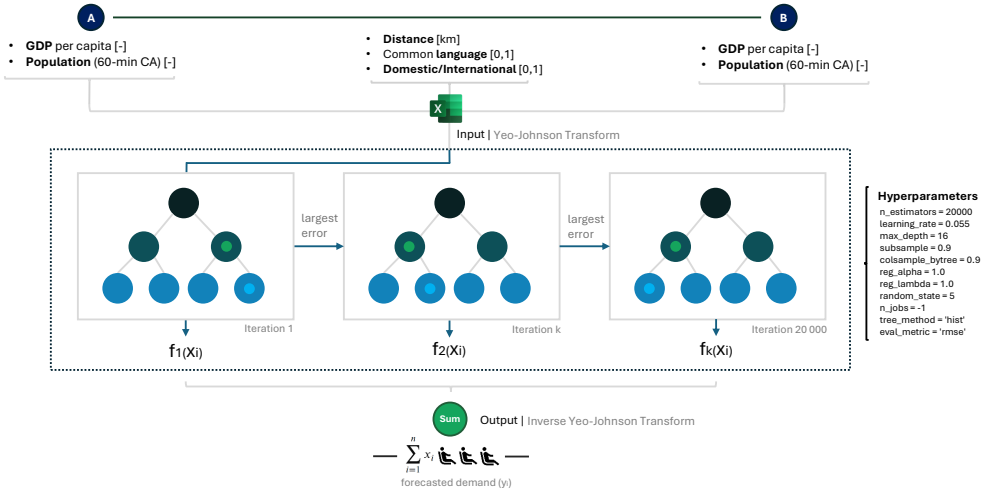

Figure 4: XGBoost Machine Learning Framework

The 5-fold distance-stratified cross-validation procedure divides the dataset into five equally sized folds while preserving the distribution of distance values across each fold (stratification by distance bins). This approach mitigates bias that could arise from uneven representation of short- versus long-haul routes in individual train/validation splits. In each iteration, the model is trained on four folds and validated on the held-out fifth fold; this process repeats five times, with each fold serving once as the validation set. The final performance metrics are computed as the average across the five validation folds. This is a vital aspect of the overall training process and provides a robust and unbiased estimate of the model's generalisation ability to completely unseen data [77].

Model performance was assessed using multiple complementary metrics: R^2 (coefficient of determination), which quantifies the proportion of variance in passenger volumes explained by the model (higher values indicate better overall fit); MAPE (Mean Absolute Percentage Error) and SMAPE (Symmetric Mean Absolute Percentage Error), which express average relative errors as percentages and facilitate intuitive interpretation in a transportation context where proportional accuracy is often prioritised; and RMSE (Root Mean Squared Error), which measures absolute error in the original units of passenger volume while penalising larger deviations more heavily. The joint evaluation of these metrics ensures a balanced view of predictive accuracy and captures both explanatory power and error magnitude across different scales and sensitivities [20].

2.1.4 Implementation of SHAP (SHapley Additive exPlanations for Machine Learning)

To enhance interpretability and address the inherent black-box nature of complex machine learning models such as XGBoost, TreeSHAP values were computed as a post-hoc explanation method. TreeSHAP is an efficient implementation of the SHAP (SHapley Additive exPlanations) [35] framework specifically tailored for tree-based models. It provides theoretically sound and locally accurate feature attributions based on cooperative game theory (Shapley values) [55, 56]. By decomposing each individual prediction into additive contributions from each input feature, TreeSHAP reveals the direction and magnitude of each feature's influence and also shows how features interact to produce the final output. This approach (visualised by Figure 5) effectively mitigates the black-box problem by transforming an opaque ensemble model into one where the contribution of every predictor can be transparently quantified and visualised for each route. The mathematical logic, underlying assumptions and supporting visualisations are outlined in Appendix B.

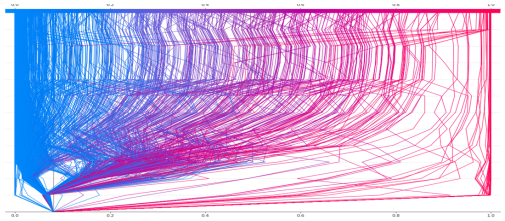

(a) SHAP feature impact tracking

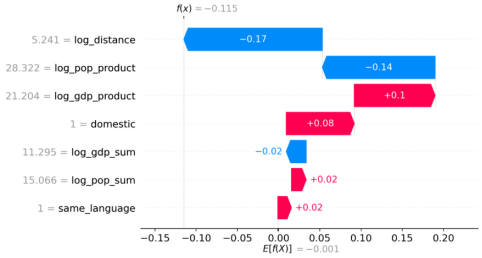

(b) SHAP quantification for an unserved route from Bologna (BLQ-PEG)

Figure 5: SHAP (SHapley Additive exPlanations for Machine Learning)

2.1.5 Induced-Demand Modelling and Sensitivity Analysis

The resulting XGBoost prediction represents the baseline annual demand $D_{\text{base}}(y_0)$ under conventional-aircraft cost structures for the reference year $y_0 = 2024$. Projected annual demand in a future year y, denoted D_y, is then obtained by applying an electrification-induced demand uplift followed by organic market growth up to the year of evaluation according to Equation 1.

$$D_y = D_{\text{base}}(y_0) \times (1 + |\varepsilon| \cdot \Delta C \cdot PT + |\varepsilon| \cdot WTP_{\text{green}}) \times (1 + g)^{y - y_0} \tag{1}$$

where ε is the short-run price elasticity of demand, ΔC is the relative reduction in direct operating costs (principally from lower energy and maintenance expenses [78]), PT is the pass-through rate of

these cost savings to ticket prices, WTP_{green} is the additional demand uplift arising from passengers' higher willingness-to-pay for zero-emission flights [89], and g is the compound annual growth rate (differentiated by domestic versus international status to reflect region-specific market dynamics) [25].

This formulation follows standard microeconomic principles used in air-transport demand modelling [47]. The short-run price elasticity of demand ε (typically negative) measures the percentage change in quantity demanded resulting from a one-percent change in ticket price. The term $|\varepsilon| \cdot \Delta C \cdot PT$ therefore directly translates the percentage fare reduction (arising from lower operating costs and passed through to passengers at rate PT), into the corresponding proportional increase in demand. The green-preference component WTP_{green} is treated analogously: even when airlines keep the ticket price unchanged, the higher willingness-to-pay for zero-emission flights effectively makes the service more attractive to passengers, acting as an equivalent virtual price reduction of the same magnitude [89]. Consequently, the same elasticity multiplier is applied to convert this preference into an additional demand uplift. The exponential term then compounds the uplifted baseline with projected organic market growth over the chosen time horizon. Parameter values are drawn from earlier studies [25, 67, 78] and applied conservatively where required to model uncertainties and ensure realistic adoption scenarios. A more detailed elaboration of the mathematical framework and underlying assumptions is provided in Appendix A.

The integrated methodology thus enables systematic, route-specific evaluation of where battery-electric regional aircraft can generate meaningful new connectivity by integrating realistic aircraft limitations, road-network-derived accessibility advantages, high-resolution market sizing, interpretable machine-learning demand estimation, and explicit representation of electrification-induced demand effects. The results of this module will be discussed in subsection 3.1, whereas its interdependencies with Module 3 and the battery-technology uncertainty study are elaborated on in subsection 3.3.

2.1.6 Synchronisation with 2040 Trans-European Transport Network (TEN-T)

Additionally, all routes actively selected and analysed within the demand forecasting tool are automatically synchronised with the planned 2040 Trans-European Transport Network (TEN-T) [10] high-speed rail corridors, which have been fully programmed into the software together with the associated projected travel times. For each candidate route, the tool performs a direct comparison between electric flight block time and the corresponding high-speed rail journey time, obtained from complementary route data [12], and issues a notification whenever a proposed electric connection overlaps with a future TEN-T corridor. Although a more rigorous modal-shift analysis using a multinomial logit model would be preferable [19], such an approach is currently not feasible because detailed service frequencies for the 2040 high-speed rail network are not yet available. The implemented synchronisation therefore represents the most practical solution for transparently flagging potential intermodal competition at this stage. Further details regarding the TEN-T integration are provided in Appendix F.

2.2 Module 2: Initial Deployment and Minimal-Infrastructure Hub-and-Spoke Network for served routes

To assess the electrification potential of currently served European routes and to design efficient initial deployment strategies for battery-electric regional aviation, a central network configuration tool for hub identification and minimal-infrastructure connectivity was developed as the primary analytical component of Module 2. This tool generates semi-range hub-and-spoke networks that maximize electrifiable passenger demand while requiring charging infrastructure at only a limited number of strategically selected hubs.

Three complementary tools were additionally created to support the core network and evaluate viable options for gradually expanding it: (i) a preliminary route feasibility assessment tool that leverages the airport characteristics embedded within the developed Geospatial Airport Information System (GAIS) in conjunction with the parametrised performance envelopes of the selected battery-electric aircraft types to quantify the exact number of electrifiable route opportunities from any given origin airport, (ii) a direct fleet-replacement analysis tool synchronised with the current active fleet deployment across the entire European route network, designed to identify the ideal electric

aircraft substitution for each served route while inducing the minimal possible alteration to existing service frequencies, and (iii) an advanced onward connectivity evaluation module that systematically analyses the electrifiability of all potential destinations reachable from each arrival airport. This facilitates an in-depth assessment of multi-leg onward network viability. While only the methodology of the primary early-phase network configuration tool will be presented in detail in this section, the additional tools for network extension, are discussed in the full study report [76] and are compactly visualised by Figure 6 as well as in Appendix I (in larger format).

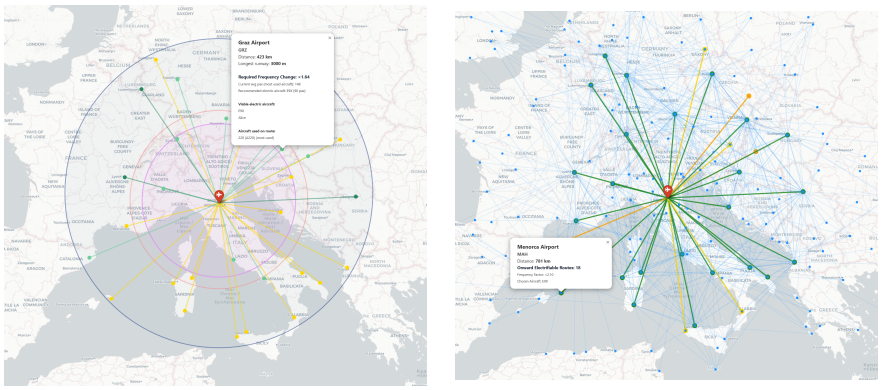

(a) Fleet replacement analysis minimising frequency change

(b) Assessment of onward electrifiable connections

Figure 6: Electrification potential assessment, extending to the early-deployment network

2.2.1 Semi-Range Hub-and-Spoke Network Design Concept

The specific hub-and-spoke network configuration tool was selected to demonstrate here as it addresses the network design challenge from a potentially unexpected, but pragmatic perspective: semi-range operations. Although limiting operations to flights close to or below half the aircraft's maximum published range may appear constraining and counter-intuitive, this focus yields interesting, implementable insights for early-phase minimal-infrastructure deployments. As demonstrated by Figure 7, by strategically concentrating charging infrastructure at a limited number of high-utilization hubs and confining spoke routes to semi-range distances, the approach achieves round-trip feasibility with charging required solely at the origin hub. This substantially mitigates the principal barriers to adoption, namely prohibitive capital expenditure, synchronized deployment timelines across many different airports for charging infrastructure installation, and regulatory complexity. This targeted infrastructure minimisation offers a viable near-term pathway to scaling a core regional electric aviation network while maintaining economic and operational realism.

Initially, the semi-range hub-and-spoke concept was anticipated to serve only a niche market segment, as concerns existed that its restricted operational scope would limit its commercial relevance. Nevertheless, applying this model to the Elysian E9X, a 90-passenger battery-electric design with a published range of approximately 800 km [30], has produced compelling results. These findings indicate a substantially larger viable market than originally projected, even indicating that energy capacity would be the most restricting factor, rather than range. The results will be examined in detail in subsection 3.2.

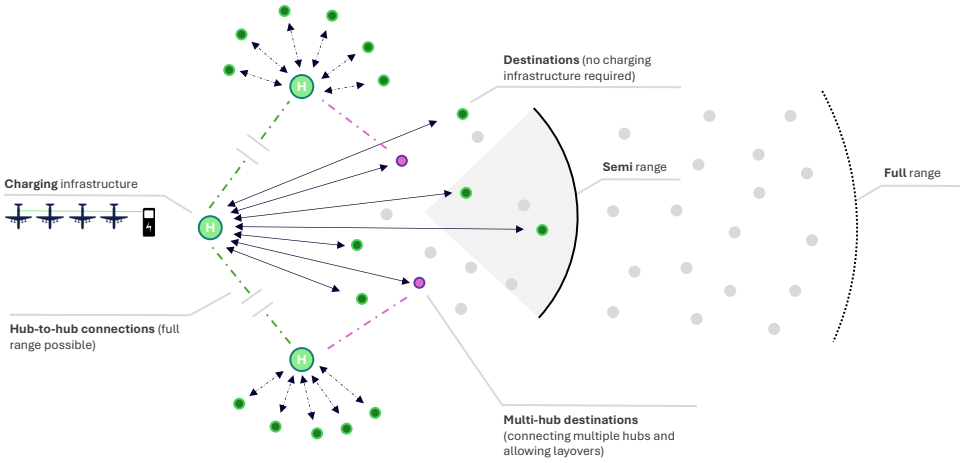

Figure 7: Minimum infrastructure hub-and-spoke network for initial deployment phase

Furthermore, the hub-centric strategy directly addresses the chicken-and-egg dilemma in electric aviation: airlines hesitate to commit aircraft without assured charging, while airports delay investment without confirmed demand. By jointly identifying high-potential hubs and the minimal set of connector airports needed for network cohesion, the tool enables stakeholders (airlines, airports, regulators, and infrastructure providers) to align early investments around a shared, economically realistic starting configuration. It thus provides a pragmatic pathway for market entry on shorter routes, deferring full-network charging upgrades until adoption matures.

2.2.2 Hub Selection and Network Generation Methodology

The tool integrates geospatial visualisation, passenger demand aggregation, and iterative graph-based connectivity enhancement. Input parameters include aircraft type (drawn from the predefined set: Vaeridion Microliner [11], Eviation Alice [5], Heart Aerospace ES-30 [8], Elysian E9X [30], or custom specification), geographic scope (one or more countries or pan-European), and the desired maximum number of hubs. For smaller-capacity aircraft, a predefined list of major conventional hubs is optionally excluded to prioritize regional airports and avoid unrealistic high-frequency operations at slot-constrained facilities dominated by medium- to long-haul traffic; this exclusion is automatically disabled for larger designs such as the Elysian E9X, and individual overrides remain available.

Analysis proceeds by computing, for every airport in the selected region with valid IATA and ICAO codes, the aggregate daily passenger demand (average passengers per direction each way, PPDEW, from SABRE origin-destination data [75]) on all routes lying within the half-range radius. Geodesic distances are calculated using WGS 84 (World Geodetic System 1984) coordinates from OurAirports [70]. Airports are ranked by this aggregated semi-range demand metric: high short-haul traffic concentration indicates strong hub potential, as a single charging location can efficiently serve numerous spokes. The top N airports ultimately form the initial hub set.

The primary output map depicts the emerging hub-and-spoke structure, as shown by Figure 8a. Hubs are shown in light green, connected by lines to semi-range destinations in dark green. Inter-hub connectivity is then assessed using the aircraft's full operational range (charging possibility at both origin and destination hubs). An optional toggle activates display of possible hub-to-hub links as dashed grey lines and highlights non-hub airports reachable from multiple hubs in purple. This reveals potential layover points that enable indirect connectivity without additional charging infrastructure.

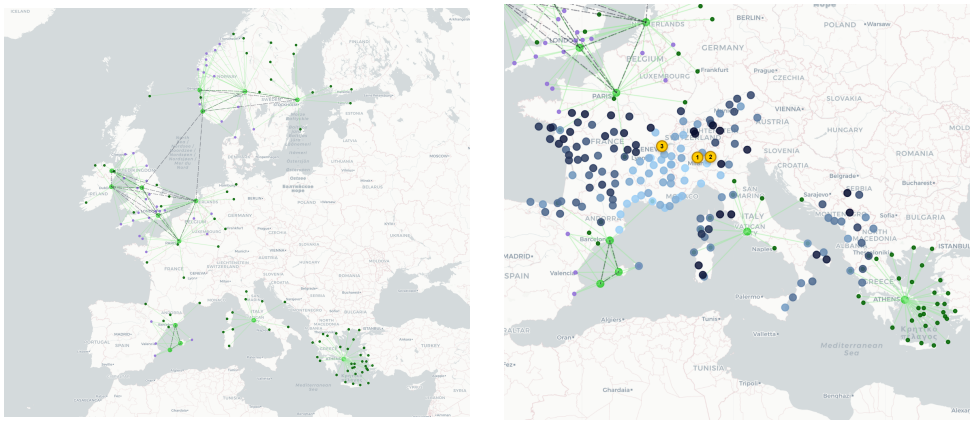

(a) Network generation for the Elysian E9X, identifying the 15 best suited hub airports in Europe (maximizing electrifiable demand)

(b) Algorithm identifying the optimal connector airports based on cluster linking capabilities and feeder traffic potential

Figure 8: Methodology of the proposed early deployment intra-European route network for the E9X, maximizing electrifiable passenger demand under limited infrastructure constraints

2.2.3 Inter-Hub Connectivity and Connector Airport Identification

Connectivity assessment frequently reveals disconnected clusters of hubs within the generated network. To progress towards a single fully connected network, an iterative Python algorithm was developed to identify suitable connector airports. These connectors are hub airports capable of linking at least two separate clusters. The algorithm ranks candidate connectors primarily by the number of clusters they bridge and secondarily by their total origin-destination passenger demand based on conventional traffic data, instead of electrifiable demand. This ranking reflects their potential role as feeder airports. The tool then generates a ranked recommendation table that presents the top candidates. Furthermore, Figure 8b displays all potential connector airports for the example case, colour-coded according to suitability using a gradient from dark navy (unsuitable) to light blue (very suitable), with the top three candidates highlighted by yellow dots together with their respective ranking numbers. The user retains full discretion to select connectors based on additional contextual factors, such as country, geographic position, connection diversity, and strategic considerations. Once a connector is added, the affected clusters are merged.

This iterative process repeats until a single fully connected network is achieved (often after adding just one or two airports, like in the example) or until the user manually terminates the procedure. Going from isolated clusters to a fully connected network is highly desirable as it offers passengers extensive geographic coverage and enables a large amount of origin-destination pairs to be travelled with zero in-flight emissions. This would often require a layover, but given the high-frequency nature of the network, waiting times would be minimal. Moreover, since charging infrastructure is required only at the designated hubs, aircraft turnaround times at the vast majority of spoke airports can be kept exceptionally low.

2.3 Module 3: R&O assessment and Battery Technology Uncertainty Framework

This module systematically identifies, evaluates, and visualises the principal barriers and enablers to the successful deployment of battery-electric regional aircraft. It places particular emphasis on identifying the relative amplitude of all risks and opportunities and on evaluating how they propagate into Modules 1, 2, and 4.

2.3.1 Risk and Opportunity Identification and Matrix Construction

Risks and opportunities were extracted from peer-reviewed literature, certification authority guidance, ongoing demonstrator programmes, and industry roadmaps [15, 48, 52, 74]. Subsequently, they were grouped into six consistent categories: technical, safety, operational, certification & regulatory, economic, and environmental. For each identified risk, the primary cause(s), most severe potential

consequence(s), and realistic mitigation measures were documented. An analogous process was applied to opportunities, with emphasis on amplification or acceleration strategies that could enhance their positive impact.

Each individual risk or opportunity is assigned a unique identifier to enable precise referencing across the analysis and diagrams. The format follows a three-part structure: category prefix (R for risk, O for opportunity), three-letter subcategory abbreviation (e.g., TEC for technical risk, SAF for safety risk), and a sequential number within that subcategory. For example, R-TEC-01 denotes the first technical risk ("Insufficient battery specific energy"), while O-ECO-01 denotes the first economic opportunity ("Lower operating costs"). This labelling allows rapid cross-referencing between text descriptions, mitigation/amplification discussions, and the visual matrices. Throughout this study, a total of 35 key risks and opportunities were identified and integrated in the matrices.

For risks, the horizontal axis represents estimated impact severity (from negligible on the left to critical on the right), while the vertical axis represents probability of occurrence (from rare at the bottom to very likely at the top). For opportunities, the horizontal axis represents potential positive impact (negligible to transformative), and the vertical axis again represents probability of realisation (rare to very likely). The nine discrete levels are formed by the matrix diagonals, producing a colour-coded severity scale that combines both dimensions into a single risk/opportunity level (1 = negligible / very low, up to 9 = critical / exceptional).

The scoring procedure adopted a deliberately neutral standpoint, equally weighting all six categories and acknowledging the inherent subjectivity in forward-looking technology assessments. Especially where probability estimates for immature systems and impact judgments can vary depending on whether the assessor prioritises operational performance, safety, environmental outcomes, or economic viability. Therefore, the matrices were reviewed by various professionals in the Aerospace Industry. Furthermore, the assigned probability and impact were always linked to scientific research where possible. Two versions of each matrix were produced: a baseline view (without mitigation/amplification) and an adjusted view (after applying the proposed strategies). Figure 9 shows the risk and opportunity matrices after the second iteration.

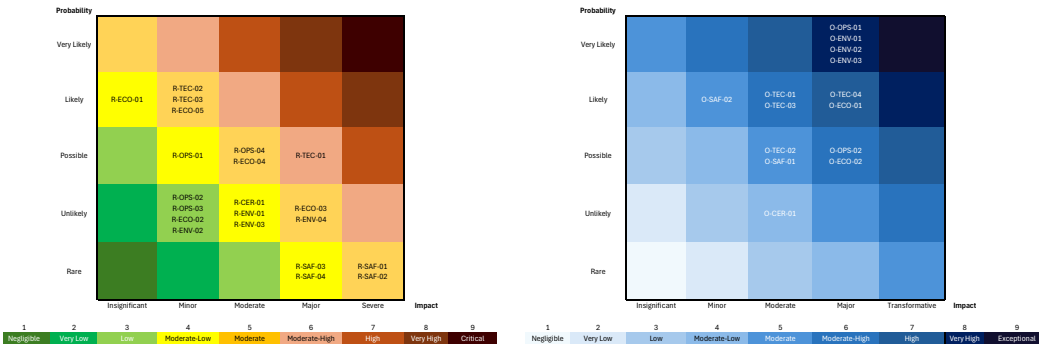

Figure 9: Risk & Opportunity Matrices after risk-mitigation and opportunity-amplification strategies

2.3.2 Battery Technology Uncertainty Framework

To address the most dominant risk identified in the risk assessment, namely R-TEC-01 (insufficient battery gravimetric energy density), a dedicated Python-based sensitivity analysis tool was developed as an extension to the initial risk evaluation process. This tool employs the aircraft design equations specifically published by Elysian [30] to model achievable range as a continuous function of pack-level gravimetric energy density, for 4 different Electric Range Factors (ERFs). The Electric Range Factor (ERF) is defined as the product of the maximum lift-to-drag ratio and the energy mass fraction (energy mass divided by maximum take-off mass, EM/MTOM). While an ERF of 12 is shown to be feasible in the design studies [90], a more conservative value of 10 was selected for this analysis. Relevant to note is that Elysian incorporates a turbo-generator in their aircraft design, however, solely

used as a backup system for loiter and diversion reserves. Therefore, the system is not used as a range extender during nominal cruise operations. Elysian's design framework was selected for this analysis as the resulting range–energy-density relationship remains structurally independent of passenger capacity variations across regional concepts [30]. Additionally, implementing a turbo-generator in a hypothetical aircraft design (as demonstrated by Elysian), results in significant additional usable range through its reserve-energy contribution. It saves significant weight and adds only a negligible fraction to total mission-related CO_2 emissions under the modelled battery-electric cruise regime.

The resulting range-versus-energy-density relationships, shown by Figure 10, serve as critical inputs to the route viability assessment in modules 1 and 2 (including served- and unserved-route forecasting) and enable quantification of how uncertainty in battery performance propagates through to network-level deployment potential and economic feasibility. These performance curves also ensure methodological consistency by providing foundational assumptions for the subsequent emissions assessment in module 4. More details are presented and discussed in the Results section.

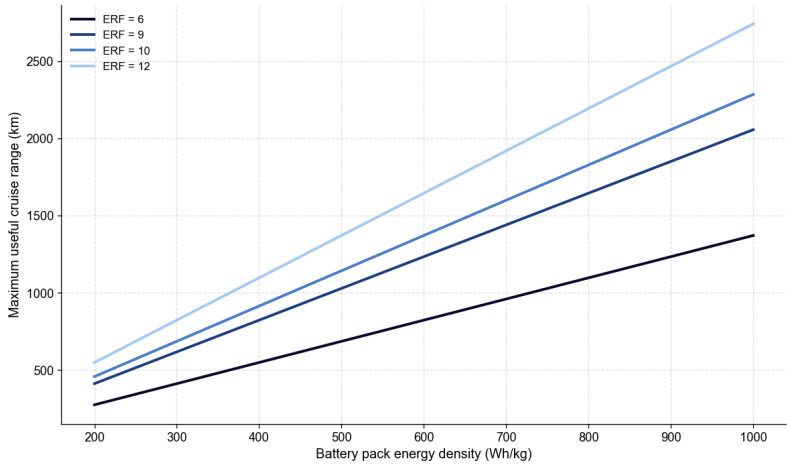

Figure 10: Energy density - range plots for various Electric Range Factors (ERF), according to Elysian's design principles [30] ,

2.4 Module 4: Environmental Impact Assessment and GHG Mitigation Potential

To evaluate the climate mitigation potential of battery-electric regional aviation within the integrated systems approach of this thesis, Module 4 links battery performance directly to theoretical sector-wide decarbonisation potential. Building upon the gravimetric energy density–range relationship developed in Module 3, this module composes it with an emission-avoidance model that translates achievable aircraft range into the theoretical share of aviation CO_2 emissions that can be displaced, as visualised by Figure 11. In doing so, it provides critical feedback to the other modules by quantifying whether advancements in battery technology can bring sector-wide emission savings to a meaningful scale.

The consequent integration with Figure 10 produces the direct relationship between pack-level battery energy density and theoretical emission avoidance potential, as shown in the results section of subsection 3.4.

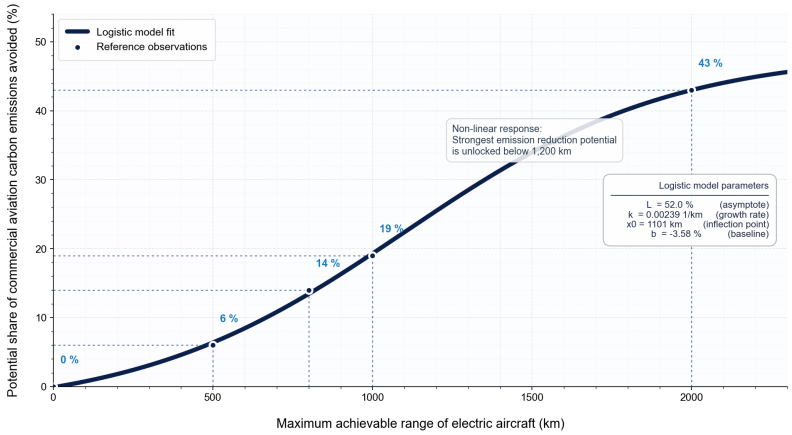

Figure 11: Sector wide CO_2 avoidance potential, constrained by achievable range of electric aircraft

In addition, a comparative energy analysis quantifies the renewable electricity demand required to produce synthetic e-fuels sufficient to power the annual operations of KLM. When benchmarked against the Netherlands' total national renewable electricity consumption, this analysis highlights the strength and potential necessity of the substantially superior energy efficiency of direct battery-electric propulsion relative to e-fuel pathways. Furthermore, a CO_2-equivalent climate impact assessment is showcased in the results section.

This module thereby closes the analytical loop of the thesis and ensures that battery-technology assumptions propagate consistently through all components while offering a system-level perspective.

3 Results

This chapter presents the main results of the four interconnected modules that form the core of this thesis. It outlines the key findings of each module while explicitly elaborating on the interdependencies between them. In particular, the battery technology uncertainty framework developed in Module 3, together with the Geospatial Airport Information System (GAIS), serves as the central mechanism that propagates consistent battery performance assumptions across demand forecasting, network design, risk assessment, and environmental impact evaluation.

3.1 Module 1: Machine-Learning Based Demand Forecasting Model and Electrification-Induced Traffic Assessment for unserved routes

This section presents the main results of the machine-learning-based demand forecasting model developed for currently unserved European routes. It also quantifies the additional traffic that could be induced by the lower operating costs and zero-emission appeal of battery-electric aircraft.

3.1.1 Performance of the XGBoost Machine Learning Model

After the 5-fold stratified cross-validation, of which a single fold visualised by Figure 12, the XGBoost model demonstrates strong predictive performance for baseline demand on currently unserved European routes. Cross-validation results yield an R^2 of 0.79 and an SMAPE of 18.7%. Table 1 summarises the complete set of performance metrics, averaged from all five folds of the entire validation procedure. These metrics indicate that the model adequately captures the underlying relationships between route characteristics and passenger volumes. The achieved accuracy provides a robust basis for the induced-demand analysis presented in the following sections.

Table 1: Performance metrics of the XGBoost base demand forecasting model (cross-validated results)

Metric	Value (mean ± std. dev.)	Description	Formula
R^2	0.7935 ± 0.0381	Proportion of explained variance	$1 - \frac{\sum(y_i - \hat{y}_i)^2}{\sum(y_i - \bar{y})^2}$
RMSE	11,770 ± 1,632	Root mean squared error	$\sqrt{\frac{1}{n}\sum(y_i - \hat{y}_i)^2}$
MAPE	25.19% ± 3.31%	Mean absolute percentage error	$100 \times \frac{1}{n}\sum\left\|\frac{y_i - \hat{y}_i}{y_i}\right\|$
SMAPE	18.69% ± 1.06%	Symmetric MAPE	$200 \times \frac{1}{n}\sum\frac{\|y_i - \hat{y}_i\|}{\|y_i\| + \|\hat{y}_i\|}$

Notes: All metrics computed via cross-validation on held-out data. RMSE in original demand units (passengers). In formulas: y_i = actual value, $\hat{y}_i$ = predicted value, $\bar{y}$ = mean of actual values, n = number of observations.

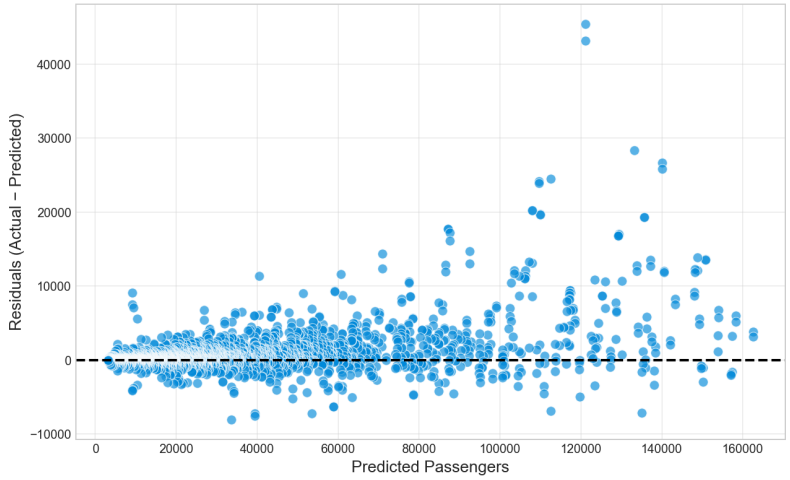

Figure 12: Validation of XGBoost Machine Learning Model (Scatter plot of residuals versus predicted demand)

3.1.2 Explanatory power of SHAP

In this study, the resulting TreeSHAP values confirmed the dominant positive influence of population and economic gravity terms (consistent with classical gravity model expectations) and the primary restraining effect of distance. Thereby, it validates the model's alignment with established theoretical principles [18, 43] and offers actionable insights into non-linear and heterogeneous route-specific effects. Notably, the restraining effect of distance (as captured by its SHAP contribution) was found to be slightly weaker (in absolute terms) compared to the effect sizes typically reported in classical gravity models or in some earlier machine learning applications to air transport [18, 27, 43]. This moderated distance penalty is largely explainable by the specific focus of the dataset on intra-European regional and short-haul routes: in such segments, where distances are generally below 1,000–1,500 km, the marginal impact of additional distance diminishes relative to longer-haul international networks, where distance effects tend to be more pronounced due to compounding factors such as fuel costs, flight time, and passenger fatigue. Furthermore, for a subset of the shortest-range segments (typically under 400–600 km), an increase in effective range can actually generate additional air travel demand by reducing competition from ground transport modes (such as high-speed rail, car, or bus) [10, 66, 69], thereby shifting modal share toward air and amplifying the positive effect of connectivity improvements. This non-linear and occasionally counter-intuitive distance–demand relationship highlights the limitations of assuming a uniform distance decay function across all route lengths in classical gravity models and demonstrates how machine learning methods, when combined with post-hoc interpretability tools like TreeSHAP [35], can capture context-dependent behavioural and competitive dynamics that traditional approaches often overlook.

3.1.3 Induced demand

Recent techno-economic studies indicate that electric propulsion can reduce direct operating costs, mainly through substantially lower energy and maintenance expenses [22, 78]. Although ALG Global projects battery-electric flight operations to reduce operating costs by 30–50 % [22], a more conservative estimate of 15-22%, is assumed in this paper, as anticipated by the Department of Science and Technology of Linköping University [78]. Adopting the midpoint value of 18.5 % and applying a conservative 70 % pass-through rate to fares, together with a short-run price elasticity of demand of -1.2 (absolute value rounded down from EU average of -1.27 [67]), provides the first component of the uplift. This is combined with an 8 % willingness-to-pay (WTP) increase for zero-emission flights. This WTP increase translates into a virtual price decrease when the ticket price is not increased and price elasticity is applied. The 8 % figure was deliberately chosen at half the lower bound reported in stated-preference surveys (16–23 %) [25]. Even though this specific research focuses on SAF (having more in-flight emissions), a cautious and conservative approach was taken. This accounts for hypothetical bias and the current lack of real-market experience with electric aircraft. Together, these effects result in a baseline electrification-induced demand increase of 25.1 % relative to conventional operations (Table 2). Sensitivity analyses show that the total uplift ranges from 17.4 % to 32.9 %, depending on the magnitude of cost reductions and the strength of the WTP effect.

Table 2: Sensitivity analysis: Projected percentage demand increase under electric aviation scenarios as a function of operating cost reductions and green-induced demand from willingness-to-pay (WTP)

Assumed operating cost reduction (%)	**Assumed green-induced demand (WTP-based) (%)**		
	4.0	8.0	12.0
15.0	17.4%	22.2%	27.0%
18.5	20.3%	**25.1%**	29.9%
22.0	23.3%	28.1%	32.9%

The interactive Python-based dashboard allows for precise, route-specific calculations of induced demand for any combination of European airports using their actual market characteristics. This flexibility of using detailed region-specific parameters is showcased by Figure 31 in Appendix E. The results presented here, however, reflect a baseline scenario using average European parameters. Furthermore, as commercial battery-electric aircraft are expected to enter service primarily in the late 2020s or early 2030s, forward-looking demand projections are more relevant than current-year estimates. The one-time 25.1% (baseline) electrification uplift is first applied to the 2026 demand forecast. Thereafter, the compound annual growth rate is applied to the full electrified demand volume (i.e., the original baseline plus the induced traffic). Table 3 demonstrates this interaction across a range of annual growth rates, holding the electrification uplift fixed at 25.1%. At a moderate average European growth rate of 2.0%, total demand by 2030 is projected to be 35.5% higher than the 2026 baseline, of which 27.2 percentage points stem from electrification. In regions with stronger growth potential, where an 8% annual growth rate is realistic, the electrification-induced contribution increases to 34.2% (compared to 2026 conventional), resulting in a total demand increase of 70.3% by 2030. Figure 13 illustrates a projected European average trajectory under the 2.2% annual growth assumption projected by EUROCONTROL [36]. This demonstrates how both the base demand as well as the induced demand accumulate alongside steady organic market expansion over the coming decade. Note that the results would be equivalent to applying the induced demand percentage after accumulation to the enhanced base demand.

Table 3: Sensitivity Analysis: Projected Percentage Increase in Aviation Demand by 2030 (from 2026 baseline, with fixed 25.1% electrification-induced uplift)

Annual Growth Rate (%)	Projected Demand Increase by 2030 (%)	
	Total	(Electrification Contribution)
0.0	25.1 %	(25.1 %)
2.0	35.5 %	(27.2 %)
4.0	46.4 %	(29.4 %)
6.0	58.0 %	(31.7 %)
8.0	70.3 %	(34.2 %)

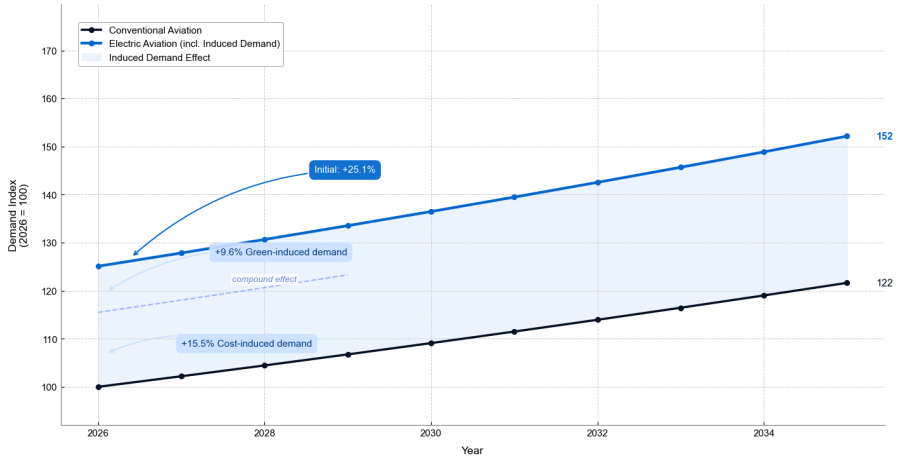

Figure 13: Projected electrification-induced demand of 25.1% (baseline), compounded with 2.2 % [36] average intra-European growth rate over the next decade

3.2 Module 2: Initial Deployment and Minimal-Infrastructure Hub-and-Spoke Network for served routes

The tool, outlined in the methodology section of this module, provides considerable flexibility in geographic scope. Users may analyse a single country, a cluster of neighbouring countries such as the Scandinavian region, or the entire European continent. Each analysis can be performed for any of the four predefined battery-electric aircraft types or, alternatively, for a user-defined custom aircraft specification that is directly linked to the battery technology uncertainty framework developed in Module 3. This functionality enables the detailed evaluation of tens of thousands of distinct scenarios. Multiple visualisations of example output networks are provided in Appendix H.

3.2.1 Suitability Analysis of the Proposed Early-Phase intra-European Hub-and-Spoke Network

For consistency with the methodology, the example case examined in this section considers the full European network with a maximum of 15 hubs and two connector airports, using the Elysian E9X as the reference aircraft. The resulting network configuration is shown in Figure 14, as well as a complementary analysis of the regions covered by this specific network. Zone A corresponds to airports in the Nordic area, which constitutes the most progressive and active region worldwide in the field of battery-electric aviation [65, 66]. This area leads global efforts through extensive research projects, industry collaborations, incentives and forward-looking policies. Norway, for instance, has established the ambitious target of achieving 100 % electric short-haul flights by 2040 [45].

Zone B corresponds to the renowned “Blue Banana” region, which represents one of the most densely populated and economically robust areas in Europe and ranks among the most dynamic regions globally [23]. Immediately adjacent lies Zone C, which encompasses Catalonia and northern Italy.

Together, Zones B and C participate in the Air-quality Initiative of Regions (AIR) [1], a collaborative platform through which the regions pool efforts to advance shared sustainability objectives.

Finally, Zone D centres on Athens. The airport is actively involved in the Greece 2.0 programme under the NextGenerationEU initiative [6]. It operates the second-largest photovoltaic installation of any airport worldwide and has already achieved its net-zero targets 25 years ahead of the global industry timeline [3].

Taken together, the generated network maximises electrifiable passenger demand while limiting charging infrastructure to a small number of strategic hubs. It connects a large number of origin-destination pairs with completely zero-emission electric flights, while the high-frequency operations and hub-only charging keep both passenger waiting times and aircraft turnaround times at spoke airports to a minimum. On top of this, the configuration concentrates on regions that combine exceptional economic strength, technical readiness, and societal commitment. The Nordic countries offer strong political support and pioneering policy targets, the Blue Banana and adjacent Mediterranean zones deliver unmatched population density and economic power, and Athens demonstrates world-leading renewable energy integration at an airport level.

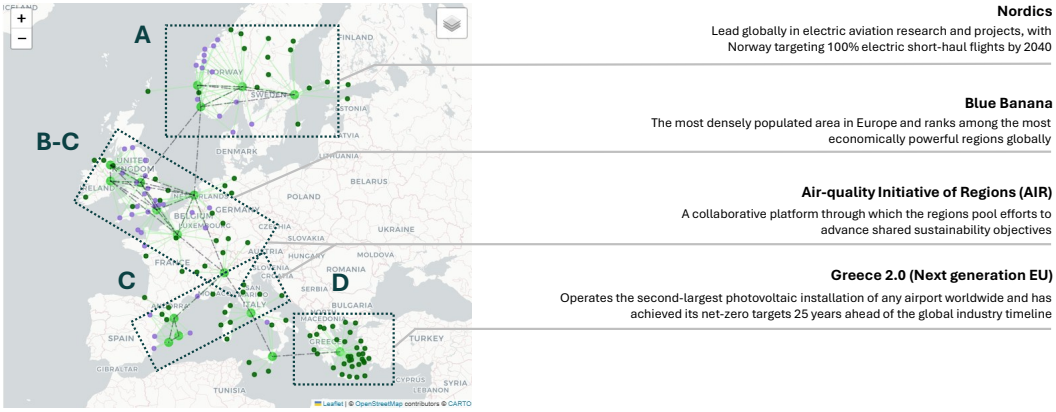

Figure 14: intra-European network analysis for the E9X, yielding maximum electrifiable passenger demand, under minimal infrastructure constraints, with a cap at 15 hub airports, complemented by 2 connector airports

3.2.2 Regional Cluster Analysis and Energy Demand Implications

An analysis of daily energy demand at the identified hub airports, presented in Appendix G, reveals relatively high requirements ranging from 207 MWh to 807 MWh per day. For context, the daily electricity consumption of a European airport with average annual passenger traffic, like Zurich (ZRH), is approximately 410 MWh [80]. These figures account for the full spectrum of processes, including ground support equipment, terminal operations, lighting, HVAC (Heating, Ventilation, and Air Conditioning) systems, baggage handling and every other imaginable energy demanding process. Consequently, the additional power demand associated with electrification is substantial. In the early deployment phase, the availability of sufficient renewable electricity may therefore prove a more critical constraint than aircraft range itself.

One might argue that spreading charging infrastructure across a larger number of airports would alleviate grid power constraints. However, the networks generated for 25 and 35 hubs (shown alongside the 15-hub case in Appendix D) demonstrate that this is not the case. The first figure in the appendix depicts the 15-hub network, with its four main clusters highlighted by white ovals. Remarkably, the additional airports selected in the 25-hub and 35-hub configurations fall almost entirely within these same four clusters. All candidate airports remain in close geographic proximity and lie within the high-potential regions identified earlier. As a result, the power demand continues to concentrate in the same regional electricity grids, offering no meaningful relief from peak loads.

Centralising infrastructure at a minimum of 15 hubs therefore delivers clear practical advantages. Concentrating megawatt-scale chargers at fewer locations allows for shared grid connection upgrades, the integration of on-site battery storage or solar arrays to smooth demand peaks, and more efficient scheduling of charging operations. In contrast, dispersing chargers across many airports would require duplicating expensive transformers, cables, and grid reinforcements at numerous sites. This would significantly increase capital costs while providing little reduction in overall grid stress. Furthermore, fewer charging locations simplify maintenance, enable the deployment of specialised technical teams, reduce downtime, and facilitate knowledge sharing among staff. On this note, Anders Forslund, head of electric aircraft manufacturer Heart Aerospace, has openly shared his concerns about an anticipated lack of technicians and ground crew capable of servicing electric aircraft. He names this as one of the key risks, potentially slowing the rollout of electric aviation in general [58]. The proposed network provides a direct solution to this concern.

Furthermore, central hubs support even lower operational costs per flight, as fixed infrastructure expenses are distributed across a larger number of daily operations rather than being spread thinly across low-frequency routes.

Ultimately, the goal is to develop charging infrastructure at all European airports. A focused hub-centric rollout in the introductory phase simply provides a realistic, cost-effective, and scalable pathway to work towards that objective. This approach offers a starting point that can be gradually expanded as the technology matures and charging infrastructure is rolled out more widely across the continent.

3.3 Module 3: R&O assessment and Battery Technology Uncertainty Framework

This section summarises the most significant risks and opportunities that remain after applying mitigation and amplification strategies in the risk and opportunity assessment. Particular attention is given to the dominant residual risk of insufficient battery gravimetric energy density. It then focuses on the battery technology uncertainty framework, which translates different pack-level energy densities into achievable range performance and analyses how this uncertainty propagates into the overall market reach and Modules 1-2.

3.3.1 Most Prominent Risks and Opportunities After Secondary Analysis

Following the application of mitigation strategies, only several risks remained at moderate (level 5) or higher on the nine-point scale. The dominant residual risk was R-TEC-01: insufficient battery gravimetric energy density. This risk consistently occupied the most critical position because of its direct influence on aircraft range, payload capability, and overall technical and economic feasibility. Other notable risks include the extensive and costly certification processes required for novel aviation battery systems, together with several battery-specific safety concerns such as crashworthiness of battery packs, potential power loss due to cell or pack failure, and hazards associated with high DC voltages. The elevated ranking of these residual risks stems primarily from their potential impact severity rather than a high probability of occurrence. In most cases, the probability can be substantially reduced through targeted mitigation strategies. This situation is analogous to a double-engine-failure scenario in conventional aircraft. While the consequences could be catastrophic, the probability remains extremely low.

On the opportunity side, the assessment highlighted several high-impact benefits. These include substantially lower operating costs, zero in-flight emissions, superior energy efficiency compared with both conventional jet fuel and synthetic e-fuels, and markedly reduced maintenance requirements. The direct impact of lower operating cost was quantified in Module 1 whereas Module 4 will elaborate on the sustainability aspects as well as the technology's high energy efficiency, and how this relates to that of its competitors.

3.3.2 Battery Technology Uncertainty Framework Integrated with GAIS for intra-European Analysis

In direct response to the most dominant risk (R-TEC-01), the results presented in this section focus on the dedicated battery technology uncertainty framework developed as an extension to the risk analysis. This framework converts assumed pack-level gravimetric energy densities into achievable operational range using the design principles of Elysian [30]. These energy-density–range relationships propagate

directly into the demand forecasting (Module 1) and network generation (Module 2) modules. As a result, every European airport's electrification potential can be assessed individually as a function of battery performance. In parallel, a large-scale analysis was conducted across the entire Geospatial Airport Information System (GAIS), which contains data for all (∼700) European airports with operational service. By computing averages over hundreds of thousands of airport-pair combinations, this approach provides broader insights into the large-scale impact of battery energy density on network viability and European-wide feasibility.

Although the tool can evaluate virtually any gravimetric energy density, the analysis presented here concentrates on three carefully selected reference values, as visualised by Figure 15. These values were chosen after a battery technology study, the full details of which appear in the complete thesis report.

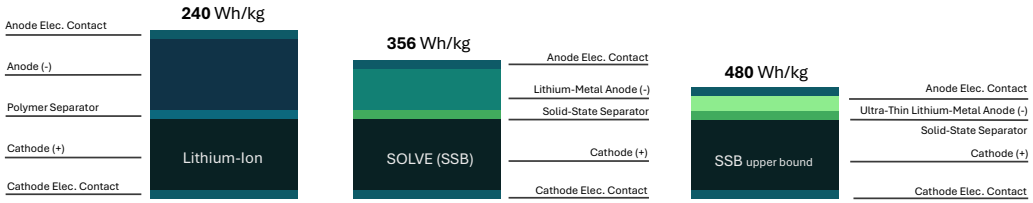

Figure 15: Battery configurations and gravimetric energy densities of three key chemistries evaluated in further analysis

The first value of 240 Wh/kg (pack level) corresponds to the near-theoretical ceiling of conventional lithium-ion batteries, the chemistry primarily in use today [71]. The second scenario, at 356 Wh/kg, reflects realistic near-term solid-state battery performance. This projection is informed by the author's attendance at a dedicated solid-state battery conference in Brussels. A prominent European initiative presented there was the SOLVE consortium [14], a Horizon Europe-funded project involving leading research institutions and Pipistrel Vertical Solutions. The latter being the manufacturer of the Velis Electro, which is the first (and, as of 2026, only) fully type-certified all-electric aircraft. SOLVE is developing advanced solid-state cells specifically tailored for aviation applications, targeting a pack-level energy density of approximately 356 Wh/kg at TRL 6 while meeting stringent safety and performance requirements for regional aircraft. This primarily include high cycle life and sufficient C-rate [14]. Further details, resulting from an interview with SOLVE's project leader (specifically held for this thesis), are outlined in the full report of this research. The third value of 480 Wh/kg represents the anticipated mid-term upper limit for solid-state battery technology, as concluded in the battery technology analysis [71].

Further substantial gains are expected to require next-generation chemistries such as lithium-sulfur or lithium-air [71]. However, these technologies still face major challenges related to material instability and limited cycle life, suggesting that commercial maturity remains many years, or even decades away [71].

Table 4 shows how the three reference gravimetric energy densities translate into theoretical useful range according to the design relations described in the methodology section (independent of passenger capacity [30]). While these range values already provide a useful first indication of market potential, integrating them with the developed Geospatial Airport Information System (GAIS) yields considerably deeper insight into the effect of incremental range improvements.

Table 4: Gravimetric battery energy density (pack level) and theoretical useful range (Elysian aircraft design principles)

Energy density (Wh/kg)	**Scenario**	**Useful range (km)**
240	Lithium-ion upper bound	548
356	SOLVE (SSB) | near-term	813
480	SSB upper bound | mid-term	1097

Notes: Assumed battery cell-to-pack ratio of 0.8.

Extending operational range naturally increases the number of reachable destination airports and the size of the population that can be served. This, in turn, expands the overall addressable market for battery-electric regional aviation. To quantify this effect systematically, the exact number of reachable destination airports was calculated for 25 discrete range segments across all the $\sim$700 operational European airports. The cumulative relationships are visualised in Figure 16a, which presents individual curves for selected major European airports alongside the European-wide average (represented by the dark navy line).

Using the 60-minute drive-time catchment areas and associated population data developed for Module 1, a parallel analysis generated the corresponding cumulative population reach as a function of range (shown in Figure 16b). In both cases, the 25 discrete data points were interpolated to produce smooth curves. These plots demonstrate that the marginal benefit of additional range differs markedly between airports, and enables highly detailed route-specific assessments where required. For the European-scale analysis conducted here, however, the average trends across all airports are employed in subsequent evaluations.

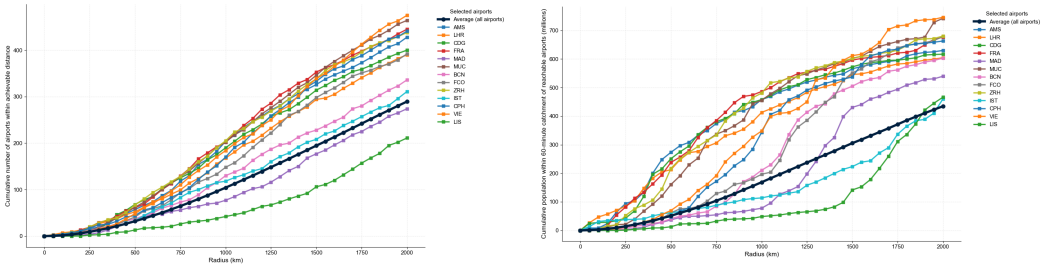

(a) Cumulative number of airports within achievable distance as a function of useful range

(b) Cumulative population within 60-minute catchment of reachable airports as a function of useful range

Figure 16: Cumulative destination and population reach plots as a function of useful range

The range-based reach curves were subsequently combined with the energy-density–range relationship. This integration expresses the average number of reachable airports and catchment population directly as functions of pack-level gravimetric energy density; the results are shown in Figure 17a and Figure 17b, respectively. In addition, Table Table 5 presents the exact average number of reachable destination airports for the three reference energy-density scenarios. The results indicate that doubling the pack energy density from 240 Wh/kg to 480 Wh/kg more than triples the average number of reachable destinations (from 37 to 120 airports). Furthermore, it shows that at the near-term solid-state battery target of 356 Wh/kg, the average European airport would be able to reach 73 destination airports within its operational electrifiable range.

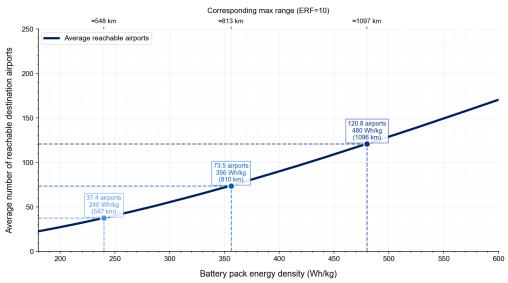

(a) Cumulative number of airports within achievable distance (European average) as a function of gravimetric energy density

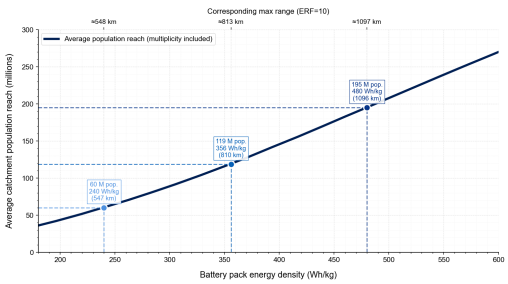

(b) Cumulative population within 60-minute catchment of reachable airports (European average) as a function of gravimetric energy density

Figure 17: Cumulative destination and population reach plots as a function of gravimetric energy density

Table 5: Theoretical market reach of battery-electric regional aviation as a function of gravimetric battery pack energy density (European average across approximately 700 operational airports)

Energy density (Wh/kg)	**Reachable destination airports (European avg.)**	**Avg. catchment population reach (60-min isochrone)**
240	37	60 M
356	73	119 M
480	120	195 M

Notes: Battery cell-to-pack ratio of 0.8 is assumed. Catchment population reach is shown in millions of inhabitants.

To further assess the practical relevance of these range-based insights for currently served routes, a parallel analysis was conducted using actual passenger traffic data from SABRE. In this case, a fixed operational range was specified and the Geospatial Airport Information System (GAIS) was queried across all European airports to identify the top 20 airports offering the highest number of served destinations (i.e., existing commercial routes) within that range. This type of evaluation can be performed for any desired range threshold.

The results for two representative thresholds (400 km and 800 km) are shown in Figure 18. Notably, the airports ranked highest under the 400 km constraint (selected purely on the basis of maximum number of served destinations within range) overlap significantly with the hubs identified in Module 2, where network optimisation was driven by aggregated passenger demand (PPDEW) under the same semi-range limitation. This strong convergence confirms that a very specific set of geographic and economic clusters (primarily in the Nordic region, the Blue Banana corridor, northern Italy/Catalonia, and the Athens area) emerges consistently as the most suitable locations for initial deployment, regardless of whether the selection criterion is potential demand or amount of connections, logically having a strong correlation.

An additional filter was applied in this served-route analysis where only routes operated by aircraft with fewer than 100 passenger seats were included. Under this constraint, 95 % of the top-ranked airports remained identical to those identified without the filter (for the 400km range). This high degree of consistency is particularly important for the introductory phase of battery-electric aviation. Early-generation electric aircraft (such as the Vaeridion Microliner, Eviation Alice, Heart ES-30, and Elysian E9X) are all designed with capacities below 100 seats [5, 8, 11, 30]. The fact that the highest-frequency, lowest-capacity routes already concentrate at these same airports means that a large share of existing services could be directly replaced by first-generation electric aircraft without requiring major changes in frequency, aircraft utilisation, or network structure. This alignment significantly reduces the commercial and operational risk of the initial rollout.

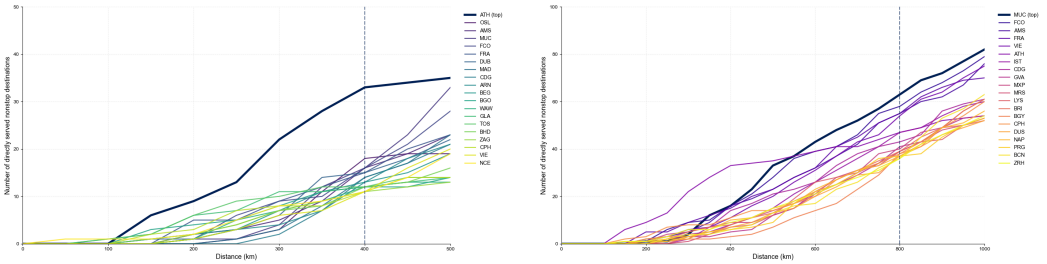

(a) Cumulative plots for the 20 intra-European airports with most served destinations within 400km range

(b) Cumulative plots for the 20 intra-European airports with most served destinations within 800km range

Figure 18: Cumulative plots for most served destinations within range thresholds of 400km and 800km

3.4 Module 4: Environmental Impact Assessment and GHG Mitigation Potential

This section presents the environmental impact assessment of battery-electric regional aviation. It starts with the theoretical sector-wide CO_2 avoidance potential as a function of gravimetric battery pack energy density and continues with derivative analysis, non-CO_2 effects, and an energy-efficiency comparison with eSAF.

3.4.1 CO_2 Avoidance Potential Under Battery Developments

Leading from the methodology described in subsection 2.4, Figure 19 illustrates the direct relationship between battery pack gravimetric energy density and the theoretical sector-wide CO_2 emission avoidance potential for European aviation. As energy density improves, longer ranges become feasible, allowing battery-electric aircraft to serve a progressively larger share of short-haul operations and thereby deliver greater decarbonisation impact at the European level.

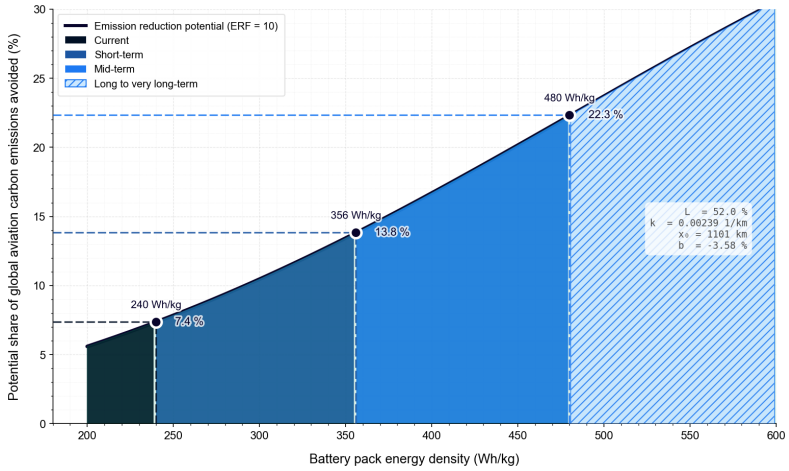

Figure 19: Sector-wide carbon avoidance potential as a function of maximum electrifiable range

Table 6 quantifies this relationship for the 3 representative scenarios, as displayed by Figure 19, as well as for a hypothetical very-long term scenario. At 240 Wh/kg, corresponding to the practical upper limit of current lithium-ion technology, up to 7.4 % of sector CO_2 emissions could be avoided. In the short term, solid-state batteries reaching 356 Wh/kg would increase this potential to 13.8 %. Looking further ahead, mid-term (upper-bound) solid-state battery technology at 480 Wh/kg offers a substantial jump to 22.3 % sector-wide CO_2 avoidance. This figure represents the expected maximum realistically achievable contribution under foreseeable battery developments. The hypothetical 800 Wh/kg scenario, which could theoretically avoid 40.6 % of emissions, would require advanced

next-generation chemistries such as lithium-air and is considered possible only in the very long term, if at all [71].

Table 6: Gravimetric battery energy density (pack level) and theoretical carbon-emission avoidance potential

Energy density (pack) (Wh/kg)	**Potential aviation carbon-emission avoidance (%)**
240	7.4
356	13.8
480	**22.3**
800	40.6

Notes: Battery cell-to-pack ratio of 0.8 is assumed

3.4.2 Derivative analysis

The derivative of the energy density–avoidance curve, presented in Figure 20, provides deeper insight into the sensitivity of decarbonisation gains to battery improvements. The left y-axis shows the instantaneous rate of change in avoidable carbon emissions (% per Wh/kg), while the right y-axis indicates the approximate additional percentage of emissions avoided for every 100 Wh/kg increase in energy density. The curve peaks sharply at approximately 479 Wh/kg. This near-perfect alignment with the projected mid-term upper limit of solid-state battery technology (480 Wh/kg) is particularly significant: it implies that the greatest marginal decarbonisation benefits will be realised precisely during the battery technology developments expected over the next 10–20 years. After this point, further energy density improvements will deliver progressively diminishing returns in terms of sector-wide CO_2 reduction.

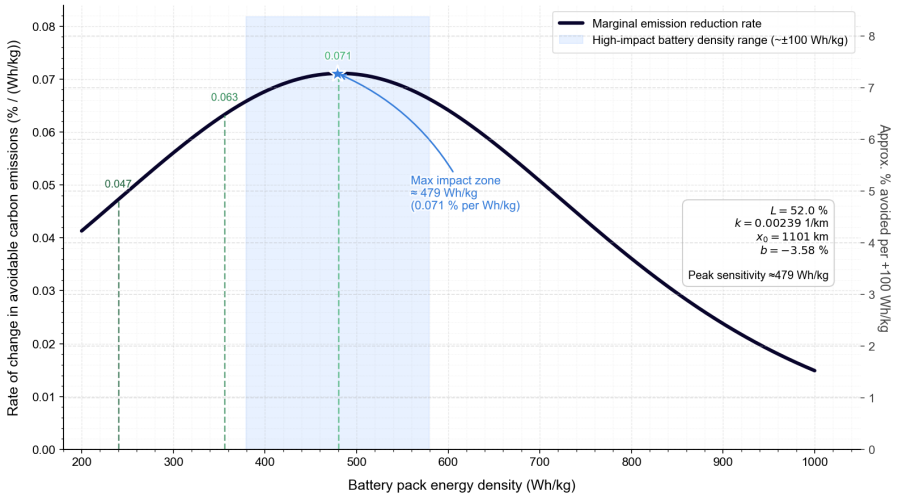

Figure 20: Derivative of the energy density - global carbon emission avoidance graph, showing the rate of change in avoidance as a function of battery developments

3.4.3 Non-CO_2 emission mitigation and CO_2-eq impact

The previous results indicate that under realistic mid-term battery performance, battery-electric aviation could avoid approximately 22.3 % of total European aviation CO_2 emissions by targeting short-haul routes. However, this figure accounts only for direct CO_2 emissions. Non-CO_2 climate effects, primarily NOx emissions at lower altitudes, are estimated to contribute a warming impact roughly equivalent to that of CO_2 itself on short-haul routes [30]. Battery-electric aircraft completely eliminate these non-CO_2 effects because there are no combustion emissions at all, whereas sustainable

aviation fuels can reduce them by only about 21 % [59]. When the full climate picture is considered, the environmental advantage of electric aviation becomes even more pronounced.

Figure 21 illustrates this point by comparing CO_2-equivalent emissions across transport modes under a 2050 projection. The reconstruction, based on external data from CE Delft [59], shows that battery-electric regional flights substantially outperform both conventional kerosene and sustainable aviation fuel options. Strikingly, on a per-passenger-kilometre basis, the overall climate impact of short-haul electric aviation can be lower than that of battery-electric cars, over the full lifecycle.

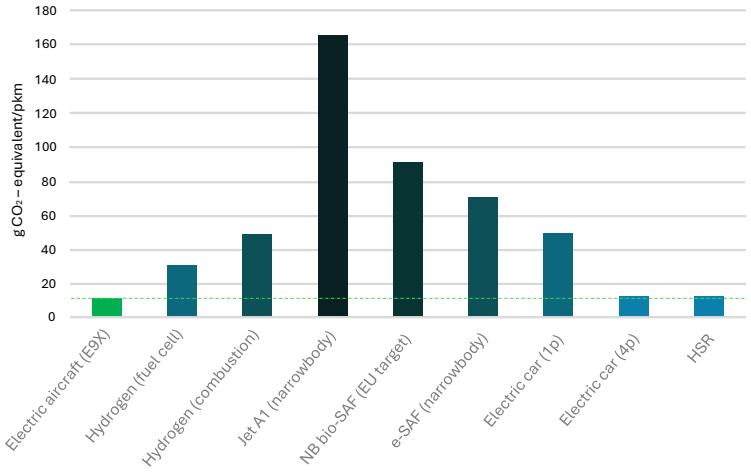

Figure 21: CO_2-equivalent emission comparison for competing transport modes (2050 projection), reconstructed with data from CE Delft [59]

3.4.4 Energy Efficiency Comparison

A final analysis, conducted as part of this thesis, quantifies and compares the energy requirements of alternative decarbonisation pathways and thereby demonstrates the efficiency advantage of direct electric propulsion. Current SAF production relies heavily on conventional pathways such as HEFA (hydro-processed esters and fatty acids) and similar biofuel routes that depend on limited feedstocks including used cooking oil, animal fats, vegetable oils, and bio waste [9]. These resources are severely constrained by sustainable biomass availability and are projected to fall far short of the increasing SAF demand, as targeted by the RefuelEU mandate [9, 59] after 2030. Consequently, the primary long-term bet in both policy and industry is on electro-sustainable aviation fuels (eSAF) [9]. These 'synthetic' fuels are produced from renewable electricity and captured CO_2.

Table 7 quantifies the renewable electricity demand required to produce sufficient e-fuels to match KLM's 2024 jet-fuel consumption. Although full replacement of an airline's entire current fleet is not a realistic near-term objective, this illustrative benchmark clearly shows the scale of the energy challenge if eSAF were to become the dominant pathway for aviation decarbonisation. Depending on the production pathway, the electricity requirement would already amount to between 2.16 and 3.05 times the Netherlands' entire renewable electricity output in 2024. This is only for a single airline and without considering future traffic growth, and for a country with a disproportionally large access to renewable electricity (mostly coming from wind). Given that renewable electricity will also be heavily demanded by many other sectors, and considering the EU's explicit ambition to significantly scale eSAF use from 2040 onward [9], these figures highlight the considerable stress that could be placed on the power system. It puts the strength of very energy-efficient transport, as offered by electric aircraft, within a broader context. Established analyses indicate that direct battery-electric propulsion is up to seven times more energy-efficient than eSAF production on short-haul missions [30]. Deploying battery electric aircraft where possible therefore offers a highly attractive pathway to relieve renewable grid pressure while also delivering superior overall climate performance.

Table 7: Theoretical electricity demand for 3330 kton e-Fuel production (KLM's 2024 fuel use [51]) compared to Netherlands' total renewable electricity consumption in 2024 (216 PJ [24]), for three e-fuel energy intensity scenarios, bounded by projections from the Royal Society [82]

Energy Intensity e-Fuel (GJ/tonne)	**Total Electricity Demand (PJ)**	**Ratio (× Netherlands' total renewable electricity use)**
140	466.20	2.16
169	562.77	**2.61**
198	659.34	3.05

Notes: Based on KLM's annual e-fuel requirement of 3330 kton and Netherlands renewable electricity consumption of 216 PJ. Total demand = quantity × intensity (in PJ). Ratio = demand ÷ 216 PJ. Middle value (169 GJ/tonne) is the average of 140 and 198 GJ/tonne. [Sources: KLM fuel data [51]; CBS renewable energy statistics [24]; The Royal Society (for eFuel production energy demand) [82]]

4 Interpretation of Results and Future Directions

Although the results of this study at first sight appear to highlight exclusively positive outcomes for battery-electric aviation, several important limitations and modelling assumptions must be considered when interpreting the findings. Firstly, the analysis relies on manufacturer-announced aircraft specifications and projected battery pack energy densities (356–480 Wh/kg) that remain subject to future technological, certification, and supply-chain developments.

Additionally, network configurations were generated under the assumption of semi-range hub-and-spoke operations with minimal charging infrastructure. They do not yet account for detailed airport-specific charging scheduling or maintenance logistics. Furthermore, the modelling approach evaluates routes largely independently and does not fully capture dynamic effects such as airline yield management, slot constraints at busy airports, or reactionary delays. Finally, while basic competition with high-speed rail via the TEN-T [10] network is included, a more detailed modal shift analysis would require future service frequency data that is not yet publicly available.

A particularly important caveat concerns the emission reduction potential. The modelling indicates that battery-electric aviation could avoid up to 22.3 % of European aviation CO_2 emissions. However, this upper-bound figure is only achievable if all flights below approximately 1,100 km are electrified, corresponding to more than 50 % of all commercial flights [30]. In reality, this scale of transformation faces multiple challenges. Conventional aircraft currently on order will remain in service for the next 25 to 30 years [73], implying that the transition will be gradual and emission reductions will materialise only over decades. However, similar slow timelines apply to the large-scale deployment of sustainable aviation fuels (SAF). On short-haul routes, however, battery-electric aviation offers a decisive advantage by completely eliminating non-CO_2 climate effects (primarily low-altitude NOx emissions), whereas SAF can reduce these effects by only approximately 20–21 % [59].

The Risk & Opportunity (R&O) analysis of this study enhances the interpretability of the findings and contributes to a realistic understanding of several operational challenges associated with scaling battery-electric aviation. Namely, a significant share of the short-haul flights suitable for electrification are currently operated by larger narrow-body aircraft with higher passenger capacities than near-term electric aircraft can realistically accommodate. Replacing these with smaller electric aircraft would likely require increased flight frequencies to maintain the same passenger throughput [44, 60]. At slot-constrained airports, this could create capacity bottlenecks [60], while airlines would face higher costs from operating more aircraft and crews [21, 44]. Although lower operating costs of electric aircraft could partially offset these economic pressures [21, 85], the net impact remains uncertain. However, such cost comparisons with today's figures are not entirely fair. Rising carbon taxes and higher conventional fuel prices are expected to increase the operating costs of fossil-based aviation over the coming decades, while sustainable aviation fuels (SAF) are also projected to remain significantly more expensive than conventional jet fuel in the near to medium term [17, 28]. Additional research will therefore be required to determine the specific thresholds for carbon pricing, SAF cost levels, and complementary policy incentives at which battery-electric aviation would become the clearly more cost-competitive choice for short-haul operations.

Current EU policies and regulations focus primarily on sustainable aviation fuels (SAF) rather than electric flight [9]. Drastic changes in policy priorities would therefore be required to incorporate

e-flight more actively into the European decarbonisation framework. Future research could usefully extend this work in several directions. First, stakeholder engagement with airports, airlines, and original equipment manufacturers should be initiated to assess common interest in focusing on a centralised network for the first deployment phase, as presented in Module 2 of this study. Second, a realistic gradual emission reduction scheme should be developed that properly accounts for the phased retirement of the current conventional fleet over its remaining lifetime. Third, further analysis is needed on the operational implications of higher flight frequencies at capacity-constrained airports and to what extent lower operating costs can mitigate the increased expenses of airlines requiring a larger number of lower-capacity aircraft. Fourth, a nested multinomial logit model could be developed to better evaluate potential modal shift behaviour once detailed service frequency data for the completed EU TEN-T high-speed rail network becomes available. Fifth, implementing GDP per capita at NUTS-3 level may improve the accuracy of the machine-learning demand model. Finally, an assessment of the most effective policies to accelerate and, where appropriate, mandate the adoption of electric aviation on short-haul routes would provide valuable guidance for decision makers.

5 Conclusion

This study demonstrates that battery-electric aviation is technically and economically feasible at a meaningful continental scale. Under projected near- to mid-term solid-state battery pack energy densities of 356–480 Wh/kg, the technology can deliver substantial decarbonisation benefits, induce additional demand, and outperform conventional aircraft and sustainable alternatives in terms of cost, emissions, and energy efficiency.

However, realising the full potential of up to 22.3 % emission avoidance will require the aviation industry to collectively commit to the complete electrification of all short-haul routes (ranges below approximately 1 100 km). Such a large-scale transition can only succeed if supported by strong, coordinated policies, targeted regulations, and well-designed incentives that actively promote battery-electric flight in parallel with Sustainable Aviation Fuels (SAF). At present, European policy frameworks remain heavily oriented toward SAF, with limited signals of near-term shifts toward electric propulsion.

Achieving this ambitious scale will therefore require close collaborative alignment and decisive action among airlines, airports, policymakers, regulators, and technology providers. The minimal-infrastructure network configuration identified in this study provides a practical and realistic starting point for this collective effort. From there, the network could be gradually expanded as battery technology continues to improve, operational experience is gained, and the necessary charging infrastructure is developed across Europe.

Regardless of the level of collaboration achieved among stakeholders, the policy tide must shift decisively to give electric aviation a fair chance and, more importantly, to enable the technology to scale to a meaningful level. Given the substantial benefits of battery-electric flight over its competitors, there is every reason to explore the most effective policies and incentives in future research.

6 Acknowledgements

The author would like to thank Ir. P.C. Roling, researcher and lecturer in Airport Operations and Operations Research at the Faculty of Aerospace Engineering, Delft University of Technology, for his valuable academic guidance and support throughout this research.

Special thanks are also extended to Koen Brinkman, Director Airport Strategies and Studies at Netherlands Airport Consultants (NACO), and Max Lomba Vrouenraets, Aviation Consultant at NACO, for their strategic insights, industry expertise, and collaboration that greatly enriched this study.

The author further acknowledges Elysian, Heart Aerospace, Eviation, and Vaeridion for (publicly) providing aircraft specifications and design principles, SABRE for the origin–destination flight data, KLM for the fuel consumption data, the SOLVE Consortium for valuable insights into solid-state battery technology, the Global Human Settlement Layer for the population data, EUROCONTROL for the growth rate projections, and OurAirports, OpenStreetMap, OpenRouteService, the European Commission, and CBS for the geospatial, airport, and statistical data used in the analysis.

References

[1] Air-Quality lnitiative of Regions (AIR). Technical report, The European Regions of Baden-Württemberg, Catalunya, Emilia-Romagna, Greater London, Hessen, Lombardia, North Rhine-Westphalia, Piemonte, Randstad, Steiermark, Veneto and Vlaanderen, Brussels, 2011.

[2] The European Green Deal. Technical report, European Comission, Brussels, 12 2019.

[3] Athens International Airport S.A. Route 2025 Roadmap. Technical report, Athens Airport, Athens, 2021.

[4] Aviation 2050 goal and the Paris agreement. Technical report, ATAG, 10 2021.

[5] Eviation Alice All Electric, All ready. Technical report, Eviation, 2021.

[6] Greece 2.0 National Recovery and Resilience Plan. Technical report, Next Generation EU, 2021.

[7] How to accelerate the implementation of electric regional aviation. Technical report, Finding Innovations to Accelerate Implementation of Electric Regional Aviation (FAIR), 2022. URL `https://fair-volta.ri.se`.

[8] Decarbonizing & democratizing air travel. Technical report, Heart Aerospace, 2024.

[9] ReFuelEU Aviation's Targets: A Feasibility Assessment. Technical report, Future Cleantech Architectures, 9 2024.

[10] Connecting Europe through High-Speed Rail. Technical report, European Commission, 2025. URL `https://citizens-initiative.europa.eu/initiatives/details/2023/000004_en`.

[11] Introducing the Microliner: A clean, cost-effective aircraft for short-haul mobility. Technical report, Vaeridion GmbH, 2025.

[12] Maps and tables containing a snapshot of the mobility service offer, state of play and planned developments, and future travel times of the EU High-Speed Rail network. Technical report, European Comission, Brussels, 11 2025.

[13] Net zero 2050: sustainable aviation fuels (SAF). Technical report, IATA, 12 2025.

[14] SOLVE: The project is well on track to develop the battery of the future. 2 2026.

[15] Mohamed Abdelhamid and Varalaxmi Gangane. Risks and benefits of sustainable aviation: factors impacting the adoption of electric planes. *Future Business Journal*, 11(1), 3 2025. doi: 10.1186/s43093-025-00468-z.

[16] Asteris Apostolidis, Stijn Donckers, Dave Peijnenburg, and Konstantinos P. Stamoulis. Electric Aircraft Operations: An Interisland Mobility Case Study. *Aerospace*, 11(3), 3 2024. ISSN 22264310. doi: 10.3390/aerospace11030170.

[17] Alexander Barke, Christian Thies, Sofia Pinheiro Melo, Felipe Cerdas, Christoph Herrmann, and Thomas S. Spengler. Comparison of conventional and electric passenger aircraft for short-haul flights - A life cycle sustainability assessment. In *Procedia CIRP*, volume 105, pages 464–469. Elsevier B.V., 2022. doi: 10.1016/j.procir.2022.02.077.

[18] Kristin Becker, Ivan Terekhov, Malte Niklaß, and Volker Gollnick. A global gravity model for air passenger demand between city pairs and future interurban air mobility markets identification. In *2018 Aviation Technology, Integration, and Operations Conference*. American Institute of Aeronautics and Astronautics Inc, AIAA, 2018. ISBN 9781624105562. doi: 10.2514/6.2018-2885.

[19] Christiaan Behrens and Eric Pels. High-Speed Rail and Air Transport Intermodal competition in the London-Paris passenger market: High-speed rail and air transport. Technical report, 2009.

[20] Alexei Botchkarev. Performance Metrics (Error Measures) in Machine Learning Regression, Forecasting and Prognostics: Properties and Typology. Technical report, 2018.

[21] Daniel Buvarp and Jennifer Leijon. Electric aircraft: a review of challenges and emerging technologies. *Discover Applied Sciences*, 8(4):444, 3 2026. ISSN 3004-9261. doi: 10.1007/s42452-026-08550-z. URL https://link.springer.com/10.1007/s42452-026-08550-z.

[22] Mario Cano, David Sabiron, and Alvaro Fernandez. How new generation aircraft could unleash great value in the short-haul market. Technical report, ALG, 5 2025.

[23] Luigi Capoani and Csaba Lakócai. Spatial dynamics of competitiveness: a comparative analysis of the Blue Banana and emerging EU regions. *Regional Statistics*, 16(1):76–99, 2026. ISSN 20648243. doi: 10.15196/RS160104.

[24] Centraal Bureau voor de Statistiek. Consumption of energy from renewable sources rises to 20 percent. Technical report, 2025.

[25] Paul Chiambaretto, Sara Laurent, Ulrike Schmalz, Mengying Fu, Audrey Rouyre, Camille Bildstein, and Anne Sophie Fernandez. Are consumers willing to pay more for green innovations? Insights from the air transport industry. *Technovation*, 137, 9 2024. ISSN 01664972. doi: 10.1016/j.technovation.2024.103079.

[26] Matthew A. Clarke and Juan J. Alonso. Forecasting the Operational Lifetime of Electric Aircraft Through Battery Degradation Modeling. In *AIAA Science and Technology Forum and Exposition, AIAA SciTech Forum 2022*. American Institute of Aeronautics and Astronautics Inc, AIAA, 2022. ISBN 9781624106316. doi: 10.2514/6.2022-1996.

[27] Shamai Cohen. A Gravity Model for Aviation Forecasting A fixed effects model for predicting global air passenger city-pair market potential. Technical report, 2016.

[28] Qiang Cui, Xu jie Sun, Xing yu Tang, Ying Zhou, Yu xin Zhang, and Ye Li. Altitude-dependent climate impacts and economic feasibility of alternative fuels in aviation from 2025 to 2050. *iScience*, 28(9), 9 2025. ISSN 25890042. doi: 10.1016/j.isci.2025.113323.

[29] Reynard De Vries, Rob E Wolleswinkel, Daniel Rosen Jacobson, Maarten Bonnema, and Sebastian Thiede. Battery performance metrics for large electric passenger aircraft. Technical report.

[30] Reynard De Vries, Rob E Wolleswinkel, Maurice F M Hoogreef, and Roelof Vos. A New Perspective on Battery-Electric Aviation, Part II: Conceptual Design of a 90-Seater. Technical report, 2024. URL https://arc.aiaa.org/.

[31] Jacob Eaton, Mohammad Naraghi, and James G Boyd. Regional Pathways for All-Electric Aircraft to Reduce Aviation Sector Greenhouse Gas Emissions. Technical report, Texas A&M University, 2024. URL https://ssrn.com/abstract=4759156.

[32] Janine Ebersberger, Leon Fauth, Ralf Keuter, Yongtao Cao, Yannik Freund, Richard Hanke-Rauschenbach, Bernd Ponick, Axel Mertens, and Jens Friebe. Power Distribution and Propulsion System for an All-Electric Short-Range Commuter Aircraft - A Case Study. *IEEE Access*, 10: 114514–114539, 2022. ISSN 21693536. doi: 10.1109/ACCESS.2022.3217650.

[33] Nina Egeli, Anders Forslund, Eric Lithun, and Maria Fiskerud. Accelerating the development of electric aviation in the Nordic countries. Technical report, Nordic Innovation, 2019.

[34] Gregor Erbach, Liselotte Jensen, Samy Chahri, and Eulalia Claros. Fit for 55 package. Technical report, European Parliamentary Research Service, 7 2024.

[35] Serap Ergün. Explaning XGBoost Predictions with SHAP value: a comprehensive guide to interpreting decision tree-based models. *New Trends in Computer Sciences*, 1(1):19–31, 4 2023. doi: 10.3846/ntcs.2023.17901.

[36] EUROCONTROL. Forecast update 2025-2031, 2025.

[37] European Comission. GHSL - Global Human Settlement Layer, 5 2026.

[38] European Regions Airline Association (ERA). Cutting emissions without cutting connections: How to make ReFuelEU work for all of Europe's airlines. Technical report, 2025.

[39] European Union. Languages, multilingualism and language rules , 5 2026.

[40] Mikael Faa. Potential network planning for electric aircraft. Technical report, Haaga-Helia University of Applied Sciences, 2022.

[41] Folium Contributors. Folium: Python data. Leaflet.js, 5 2026.

[42] Stephen Glinski, Bijan Fazal, Evan D Harrison, Mayank V Bendarkar, Taylor Fields, and Elena Garcia. An MBSE Framework to Identify Regulatory Gaps for Electrified Transport Aircraft. *IEEE Transportation Electrification Conference & Expo (ITEC)*, 2022.

[43] Tobias Grosche, Franz Rothlauf, and Armin Heinzl. Gravity models for airline passenger volume estimation. *Journal of Air Transport Management*, 13(4):175–183, 7 2007. ISSN 09696997. doi: 10.1016/j.jairtraman.2007.02.001.

[44] David Hyde, Raphael Berz, Saprina Carter, Jonathan Li, Adam Mitchell, Robin Riedel, and Michael Saposnik. Target True Zero: Delivering the Infrastructure for Battery and Hydrogen-Powered Flight. Technical report, McKinsey & Company, 2023.

[45] Institute of Transport Economics Norwegian Centre for Transport Research. Accelerating the phase in of electric aircraft in Norway Possible societal impacts and policy instruments. 2021. ISSN 1851/2021. URL `www.toi.no`.

[46] International Monetary Fund World Economic Outlook. List of European countries by GDP per capita, 5 2025.

[47] InterVISTAS. Estimating Air Travel Demand Elasticities. Prepared for IATA. Technical report, 2007.

[48] Arun Karwal and Marijn Giesberts. Safety aspects of electric flight operations. Technical report, NLR, 2022.

[49] Hyun D. Kim, Aaron T. Perry, and Phillip J. Ansell. A Review of Distributed Electric Propulsion Concepts for Air Vehicle Technology. In *2018 AIAA/IEEE Electric Aircraft Technologies Symposium, EATS 2018*. Institute of Electrical and Electronics Engineers Inc., 11 2018. ISBN 9781624105722. doi: 10.2514/6.2018-4998.

[50] Will Koehrsen. A Conceptual Explanation of Bayesian Hyperparameter Optimization for Machine Learning. Technical report, 2018.

[51] Koninklijke Nederlandse Luchtvaart Maatschappij N.V. KLM Annual Report 2024. Technical report, 2024.

[52] Nasa V Kurt Papathakis, Alaric Sessions, Jacobs Technology Phillip Burkhardt, and David Ehmann. A NASA Approach to Safety Considerations for Electric Propulsion Aircraft Testbeds. Technical report, NASA, 2017. URL `www.nasa.gov`.

[53] Martin Lindberg and Jennifer Leijon. Electrifying aviation: Innovations and challenges in airport electrification for sustainable flight, 6 2025. ISSN 26667924.

[54] Lennart Lobitz, Alexander Hahn, Daniel Vogt, Tim Luplow, Peter Michalowski, Sebastian Heimbs, and Georg Garnweitner. Conceptual Challenges for Crashworthy Battery-Electric Commercial Aircraft: Review. *the American Institute of Aeronautics and Astronautics*, 2025.

[55] Scott Lundberg and Su-In Lee. A Unified Approach to Interpreting Model Predictions. 11 2017. URL `http://arxiv.org/abs/1705.07874`.

[56] Scott M. Lundberg, Gabriel G. Erion, and Su-In Lee. Consistent Individualized Feature Attribution for Tree Ensembles. 3 2019. URL `http://arxiv.org/abs/1802.03888`.

[57] Tove Lundberg. Accessibility study for electric aviation. Technical report, Nordic Innovations, 2022.

[58] Kevin McGwin. How short-haul Arctic air routes could help electric passenger planes get off the ground, 10 2021.

[59] Christiaan Meijer, Koen van der Griesen, Geert Bergsma, Jan van de Pol, Joeri Vendrik, Reinier van der Veen, and Stefan Grebe. Climate Change Impact Analysis of Electric Aviation. Technical report, CE Delft, 1 2025.

[60] Jayant Mukhopadhaya and Brandon Graver. Performance Analysis of Regional Electric Aircraft. Technical report, The International Council on Clean Transportation (ICCT), 2022. URL `www.theicct.orgcommunications@theicct.org`.

[61] NACO. Scheduled global air-services and fleet assignment. Technical report, NACO, Delft, 2025.

[62] National Aviation Authorities Network. Roadmap for advanced air mobility aircraft type certification. Technical report, 2025.

[63] Andy Navarette. Understanding the greenhouse gas emissions of different SAF pathways. Technical report, International Council On Clean Transportation, 10 2025.

[64] Jon Nazca. IATA backs call by European airlines to soften green fuel mandate, 3 2025.

[65] Nordic Network for Electric Aviation. Accelerating the development of electric aviation , 2026.

[66] Nordregio. Ten-year Regional Outlook: Future Perspectives for Electric Aviation in the Nordic Region. Technical report, 2024.

[67] Katrin Oesingmann and Katrin Kölker. Price Elasticities in Aviation: Novel Estimates from Structural Gravity Modelling and Instrumental Variables Approach. In *Transportation Research Procedia*, volume 94, pages 58–66. Elsevier B.V., 2026. doi: 10.1016/j.trpro.2026.01.007.

[68] ORS Contributors. Open Route Service (ORS), 5 2026.

[69] OSM Contributors. OpenStreetMap (OSM), 5 2026.

[70] OurAirports Contributors. OurAirports airport database, 5 2026.

[71] Tavish Pattanayak and Dimitri Mavris. Battery technology for sustainable aviation: a review of current trends and future prospects. *Applied Energy*, 397, 11 2025. ISSN 03062619. doi: 10.1016/j.apenergy.2025.126356.

[72] Prakash Prashanth, Jad Elmourad, Carla Grobler, Stewart Isaacs, Syed Shayan Zahid, James Abel, Christoph Falter, Thibaud Fritz, Florian Allroggen, Jayant S. Sabnis, Sebastian D. Eastham, Raymond L. Speth, and Steven R.H. Barrett. Near-zero environmental impact aircraft. *Sustainable Energy and Fuels*, 8(20):4772–4782, 7 2024. ISSN 23984902. doi: 10.1039/d4se00419a.

[73] Antonia Rahn, Melissa Schuch, Kai Wicke, Benjamin Sprecher, Clemens Dransfeld, and Gerko Wende. Beyond flight operations: Assessing the environmental impact of aircraft maintenance through life cycle assessment. *Journal of Cleaner Production*, 453, 5 2024. ISSN 09596526. doi: 10.1016/j.jclepro.2024.142195.

[74] Jayaraj Rane, Bharatkumar Solanki, Scott Cary, Prateek Joshi, and Subhankar Ganguly. Overview of Potential Hazards in Electric Aircraft Charging Infrastructure. Technical report, National Renewable Energy Laboratory, 2023. URL `www.nrel.gov/publications.`

[75] SABRE. Inter-European passenger demand data. Technical report, SABRE, 2024.

[76] Thijs Savelberg. Assessing the feasibility and scalability of short-haul battery-electric aviation in Europe: Coupling ML-based demand forecasting, network modelling and GHG mitigation potential under battery constraints (extended report). 2026.

[77] Scikit-learn developers. Cross-validation: evaluating estimator performance, 2025.

[78] Kawthar Shahwan. Operating Cost Analysis of Electric Aircraft on Regional Routes. Technical report, Linkopings Universitet, 12 2021.

[79] Donald L. Simon and Joseph W. Connolly. Electrified Aircraft Propulsion Systems: Potential Failure Modes and Failure Mitigation Strategies. *International Council on Systems Engineering (INCOSE) Foundation, NASA Headquarters*, 2019.

[80] Sleiman Sleiman and Mohamed Ouf. A review on energy practices and indoor environmental quality (IEQ) of airports, 6 2025. ISSN 03601323.

[81] Junzi Sun, Xavier Olive, and Daniel Delahaye. Evaluating Aviation Emission Inefficiencies and Reduction Challenges with Electric Flights. Technical report, Faculty of Aerospace Engineering, Delft University of Technology, the Netherlands, 2019.

[82] The Royal Society. Net zero aviation fuels: resource requirements and environmental impacts. Technical report, 2023.

[83] Mari Tuominem. 'Fit for 55' legislative package: ReFuel EU Aviation. Technical report, European Parliamentary Research Service, 12 2021.

[84] Bruno Vanzieleghem. Next-generation batteries to enable electric aviation. Technical report, International Civil Aviation Organization, 2022. URL `https://thebarentsobserver.com/en/travel/2020/03/`.

[85] Muthu Venkatesh, Amit Kumar Thakur, Lovi Raj Gupta, and Rajesh Singh. A Comprehensive Review of Concepts, Benefits, and Challenges of a Battery-Powered Aircraft. Technical report, 2024.

[86] Stefany Villacis, Antonia Rahn, Urte Brand-Daniels, and Thomas Vogt. Towards Sustainable Aviation: End-of-Life Scenarios for Lithium-Ion Batteries used in Hybrid Electric Aircraft. In *Procedia CIRP*, volume 135, pages 1252–1258. Elsevier B.V., 2025. doi: 10.1016/j.procir.2024.12.134.

[87] Nicolas F M Wahler, Daigo Maruyama, and Ali Elham. Credibility-Based Multidisciplinary Design Optimization of Hybrid-and Fully-Electric Aircraft. Technical report, 2023.

[88] Sanford Weisberg. Yeo-Johnson Power Transformations. Technical report, 2001. URL `http://www.stat.umn.edu/arc.`

[89] Nicole Wendt, Gorm Kipperberg, and Henrik Lindhjem. Consumer willingness to pay for emission reduction in air travel: A meta-analysis. *Transportation Research Part D: Transport and Environment*, 134, 9 2024. ISSN 13619209. doi: 10.1016/j.trd.2024.104347.

[90] Rob E Wolleswinkel, Reynard De Vries, Maurice F M Hoogreef, and Roelof Vos. A New Perspective on Battery-Electric Aviation, Part I: Reassessment of Achievable Range. Technical report, 2024. URL `https://arc.aiaa.org/`.

[91] Renju Aleyamma Zachariah, Sahil Sharma, and Vijay Kumar. Systematic review of passenger demand forecasting in aviation industry. *Multimedia Tools and Applications*, 82(30):46483–46519, 12 2023. ISSN 15737721. doi: 10.1007/s11042-023-15552-1.

[92] Aleksandra Zieminska-Stolarska, Mariia Sobulska, Daniel Izquierdo, Deborah Neumann Dela Cruz, Monika Pietrzak, and Ireneusz Zbicinski. Life Cycle Assessment of Hybrid-Electric Aircraft Technologies - A Review, 2025. ISSN 21693536.

A Mathematical Formulation of the Induced-Demand Forecasting Model

The demand forecasting model augments a standard compound growth projection with two mechanisms by which electric propulsion is expected to increase air passenger demand: lower ticket prices from reduced operating costs and a willingness-to-pay (WTP) premium for zero-emission and low-noise attributes. Both effects are channelled through the price elasticity of demand. The equation reads:

$$D_y = D_{\text{base}(y_0)} \times [1 + |\varepsilon| \cdot \Delta C \cdot \text{PT} + |\varepsilon| \cdot \text{WTP}_{\text{green}}] \times (1+g)^{y-y_0} \tag{2}$$

where the variables are as defined in the main text.

Baseline demand $D_{\text{base}(y_0)}$ in the reference year y_0 is first projected forward using the exogenous compound growth factor $(1+g)^{y-y_0}$, where g denotes the assumed constant annual growth rate. The term in square brackets then captures the additional demand uplift attributable to electric propulsion.

This uplift is derived from the constant-elasticity demand function. The absolute value of the price elasticity $|\varepsilon|$ of 1.2 (rounded down from European average of 1.27 [67]) converts any effective reduction in ticket price into a proportional increase in quantity demanded.

The first component stems from operating cost savings. Literature indicates that electric propulsion can reduce operating costs by 15–21%, primarily through lower energy costs and reduced maintenance requirements [78]. The central value $\Delta C = 0.185$ adopted here is the arithmetic mean of this range. Not all savings are passed on to passengers; the pass-through rate PT (0.70) reflects competitive realities in which airlines retain part of the benefit. The product $\Delta C \cdot \text{PT}$ therefore represents the expected net price reduction, which, when multiplied by $|\varepsilon|$, yields the induced demand increase.

Although literature reports willingness-to-pay premiums for green aircraft attributes between 16% and 23% of the ticket price [25], a more conservative baseline value of $\text{WTP}_{\text{green}} = 0.08$ (8%) is adopted. This corresponds to half the lower bound of the reported range and accounts for uncertainties inherent in stated-preference surveys, including potential hypothetical bias and limited real-market experience with electric aircraft. This premium is treated as a virtual price decrease: the additional utility from a zero-emission, low-noise aircraft is economically equivalent to receiving a discount of $\text{WTP}_{\text{green}}$ on a conventional flight. The same elasticity therefore generates a further demand stimulus via the term $|\varepsilon| \cdot \text{WTP}_{\text{green}}$.

The two effects are added inside the brackets as they operate through the same elasticity channel. The resulting multiplier gives the total demand uplift relative to the exogenous growth path, as visualised by Figure 22 (not on scale as CAGR is dependent on the evaluation year). All parameters are held constant over the forecast horizon for analytical transparency, but may vary depending on the specific region. The values discussed in this appendix correspond to the baseline European average scenario.

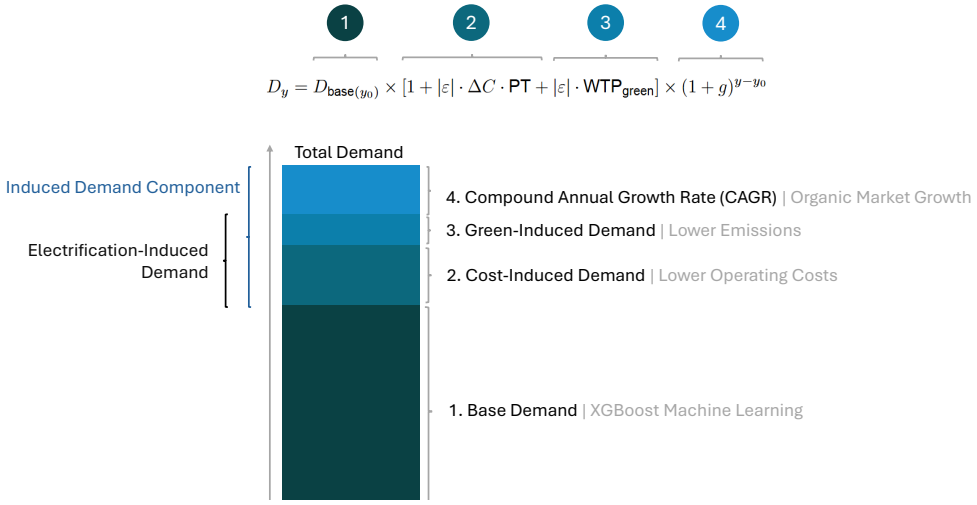

Figure 22: Induced demand components and CAGR, extending to baseline demand (not on scale)

B TreeSHAP Interpretability Analysis: Methodology, Mathematical Background, and Supporting Visualisations

The core logic behind SHAP [55, 56] is to explain the model prediction $f(\mathbf{x})$ using an additive feature attribution model g:

$$g(\mathbf{z}') = \phi_0 + \sum_{i=1}^{M} \phi_i z'_i, \tag{3}$$

where

- ϕ_0 is the base value, i.e., the expected model output $\mathbb{E}[f(\mathbf{x})]$ over the background dataset,
- $\phi_i \in \mathbb{R}$ denotes the SHAP value (contribution) of feature i,
- $\mathbf{z}' \in \{0,1\}^M$ is a binary vector indicating whether feature i is observed ($z'_i = 1$) or masked ($z'_i = 0$),
- M is the total number of features.

This formulation satisfies three key properties:

- **Local accuracy**: $g(\mathbf{x}') = f(\mathbf{x})$,
- **Missingness**: $z'_i = 0 \phi_i = 0$,
- **Consistency**: if a feature's marginal contribution never decreases when the model changes, its SHAP value does not decrease.

The SHAP value for feature i is uniquely defined as the Shapley value from cooperative game theory:

$$\phi_i(f, \mathbf{x}) = \sum_{S \subseteq N \setminus \{i\}} \frac{|S|!\,(M - |S| - 1)!}{M!} \Big[f_{\mathbf{x}}(S \cup \{i\}) - f_{\mathbf{x}}(S) \Big], \tag{4}$$

where $N = \{1, \ldots, M\}$ is the set of all features, S is any subset not containing i, and the conditional model output is defined as

$$f_{\mathbf{x}}(S) = \mathbb{E}\big[f(\mathbf{x}) \mid \mathbf{x}_S \big]. \tag{5}$$

For tree-based models such as XGBoost, the **TreeSHAP** algorithm computes these values exactly and efficiently with computational complexity $\mathcal{O}(TLD^2)$, where T is the number of trees, L the maximum number of leaves per tree, and D the maximum tree depth.

In this study, SHAP values were computed using `shap.TreeExplainer` on the final XGBoost model with the following feature set (visualised by Figure 23:

```
['log_distance', 'log_gdp_product', 'log_pop_product', 'domestic',
 'same_language', 'log_gdp_sum', 'log_pop_sum']
```

Global interpretability is provided by the SHAP summary (beeswarm) plot, which ranks features by their mean absolute SHAP value and illustrates the direction and magnitude of each feature's impact. Higher values of `log_pop_product` and `log_gdp_product` consistently increase predicted demand, while `log_distance` exerts a slightly negative effect.

Local explanations for individual predictions (e.g., specific routes) are visualised by Figure 24a and Figure 24b, which decompose a single prediction according to:

$$f(\mathbf{x}) = \phi_0 + \sum_{i=1}^{M} \phi_i. \tag{6}$$

Feature interactions are quantified via SHAP interaction values:

$$\Phi_{i,j} = \sum_{S \subseteq N \setminus \{i,j\}} \frac{|S|!\,(M - |S| - 2)!}{2(M-1)!} \Big[\Delta_{ij}(S)\Big], \tag{7}$$

where $\Delta_{ij}(S) = f_{\mathbf{x}}(S \cup \{i,j\}) - f_{\mathbf{x}}(S \cup \{i\}) - f_{\mathbf{x}}(S \cup \{j\}) + f_{\mathbf{x}}(S)$.

The SHAP analysis confirms that the population and economic gravity terms (`log_pop_product`, `log_gdp_product`) are the dominant positive drivers of predicted demand, while great-circle distance acts as the primary constraining factor. These results reveal non-linear effects and interactions that align with classical gravity theory and demonstrate how the XGBoost model captures complex dependencies in the data.

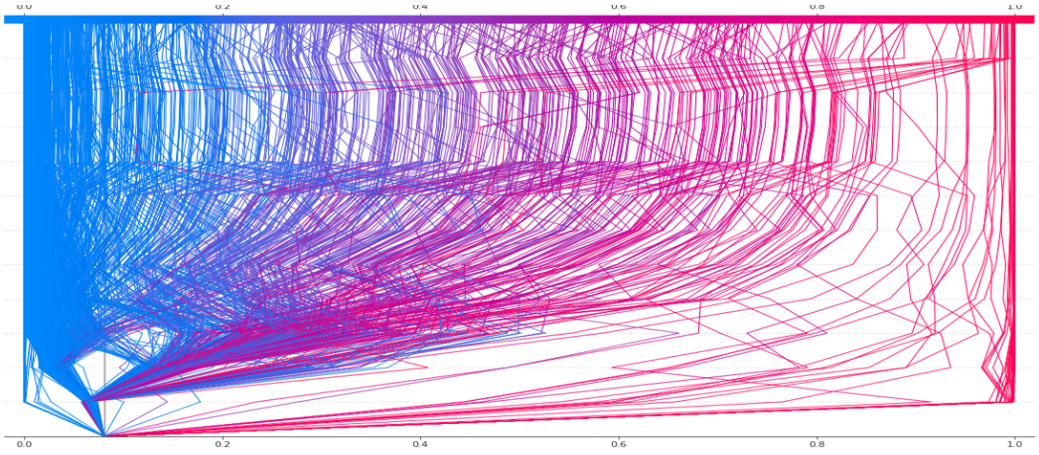

Figure 23: Game-based inspired tracking of a variable's individual contribution to the output (SHAP) [35]

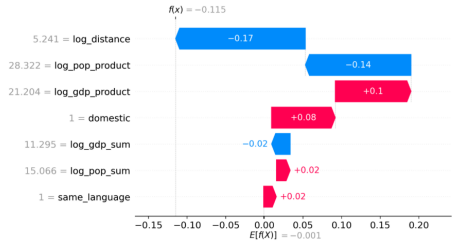

(a) Absolute contributions of the variables implemented in the proposed ML-model for an unserved route from Bologna (BLQ) to Perugia (PEG)

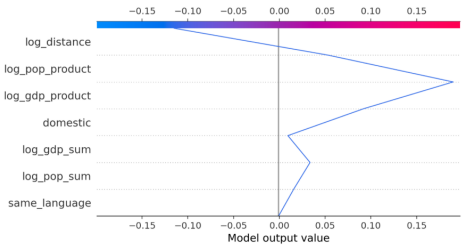

(b) Cumulative path of the variable contributions, leading to the forecasted demand for BLQ-PEG

Figure 24: SHAP plots for BLQ-PEG

C Catchment Area Delineation and Population Reach Computation Methodology

The road network is modelled as a directed, weighted graph

$$G = (V, E), \tag{8}$$

where

- V is the set of vertices (road junctions, intersections, and airport locations),
- $E \subseteq V \times V$ is the set of directed edges (road segments).

Each edge $e = (u, v) \in E$ has a non-negative weight $w(e)$ representing the estimated travel time in minutes from u to v, derived from OpenStreetMap attributes via OpenRouteService (ORS) driving profiles.

The *shortest-path travel time* $d(s, v)$ from airport (source) $s \in V$ to vertex $v \in V$ is

$$d(s, v) = \min_{\pi : s \rightsquigarrow v} \sum_{e \in \pi} w(e), \tag{9}$$

where $\pi : s \rightsquigarrow v$ denotes any path from s to v. Computation uses optimised Dijkstra variants (with contraction hierarchies or A*).

The 60-minute drive-time isochrone around airport s is the set

$$I(s, T) = \big\{ v \in V \;\big|\; d(s, v) \le T \big\} \quad \cup \big\{ p \in \mathbb{R}^2 \;\big|\; \exists (u, v) \in E,\ p \text{ on edge } (u, v),\qquad d(s, u) + w'(u, p) \le T \big\}, \tag{10}$$

with $T = 60$ minutes and $w'(u, p)$ the linearly interpolated travel time from u to point p on the edge.

The boundary $\partial I(s, T)$ is represented as a closed polygon generated by ORS [68] through contouring of network points at exactly travel time T, as displayed by Figure 25.

In this study, isochrones $I(s, 60)$ were computed using the OpenRouteService API [68] with the default driving profile. Catchment areas were then enriched by intersecting the resulting polygons with 100 m resolution gridded population data (Global Human Settlement Layer [37]) and aggregating the population within each polygon. This network-based approach provides a realistic and more accurate alternative to simple circular buffers.

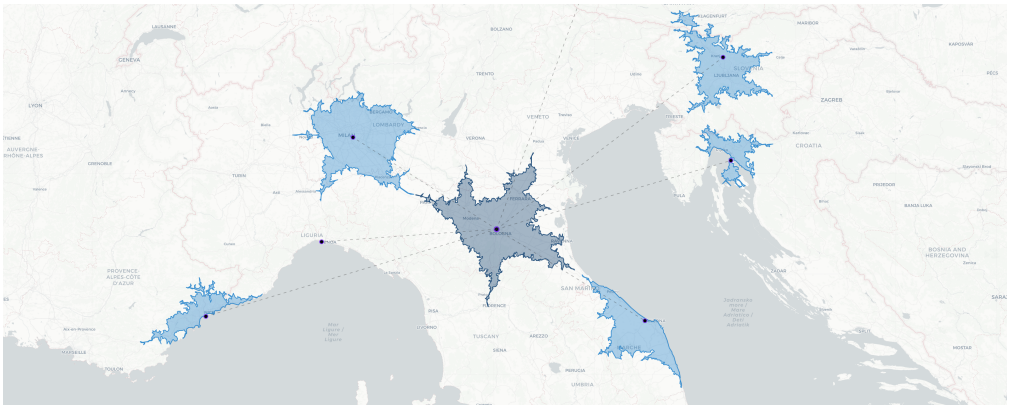

Figure 25: 60-minute isochrone catchment area analysis for potential routes from Bologna Airport (BLQ) ,

D Additional Hub-and-Spoke Network Configurations (25- and 35-Hub Sensitivity Cases)

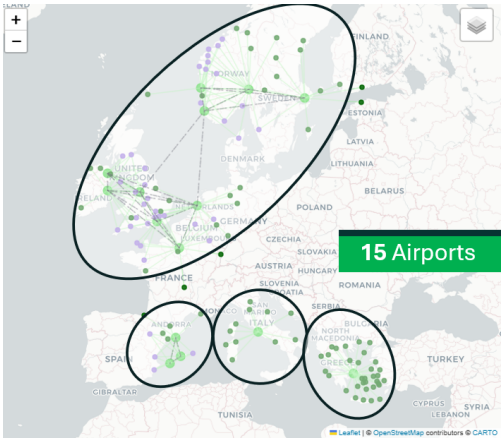

Figure 26: Proposed network for the input variables described in module 2, solving for 15 hub airports

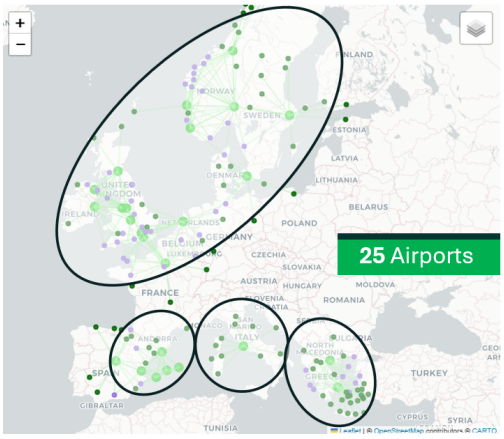

Figure 27: Proposed network for the input variables described in module 2, solving for 25 hub airports

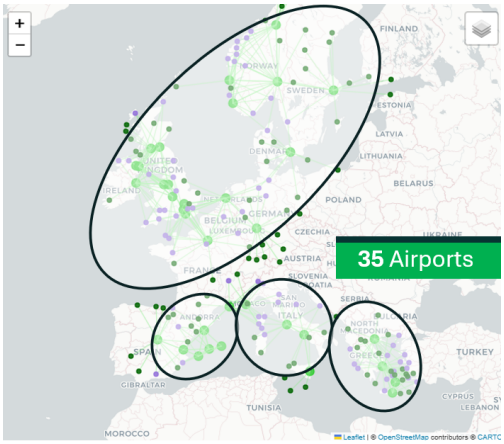

Figure 28: Proposed network for the input variables described in module 2, solving for 35 hub airports

E Interactive Dashboard User Interface and Input Parameters (Demand Forecasting Tool)

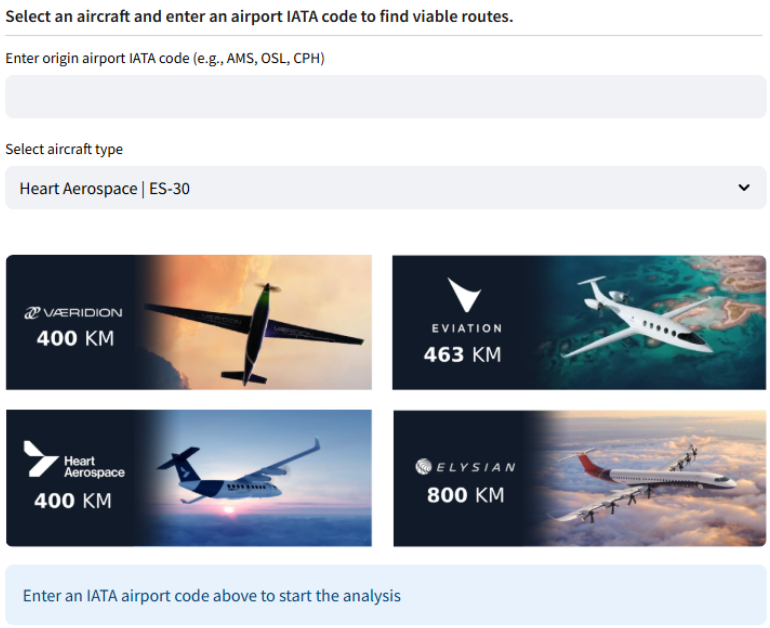

Figure 29: Electric aircraft and airport selection menu of module 1

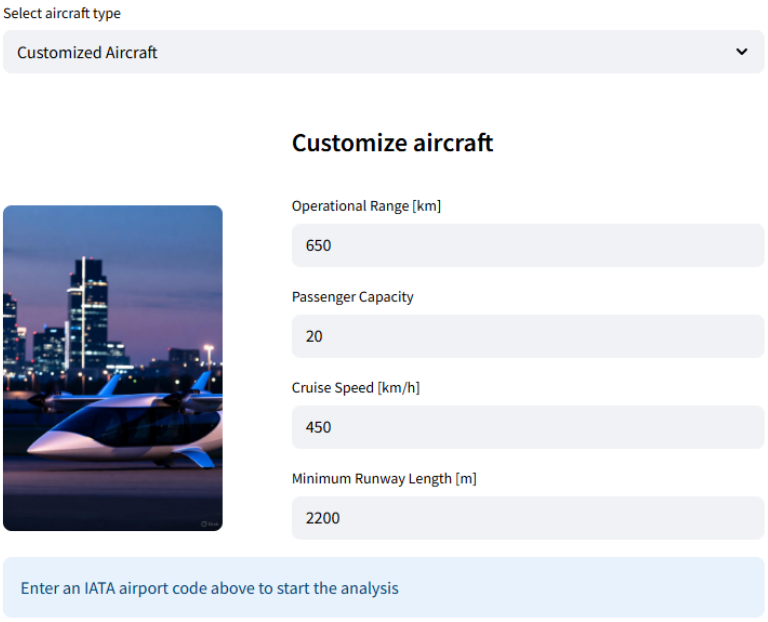

Figure 30: Customized electric aircraft option for sensitivity analysis

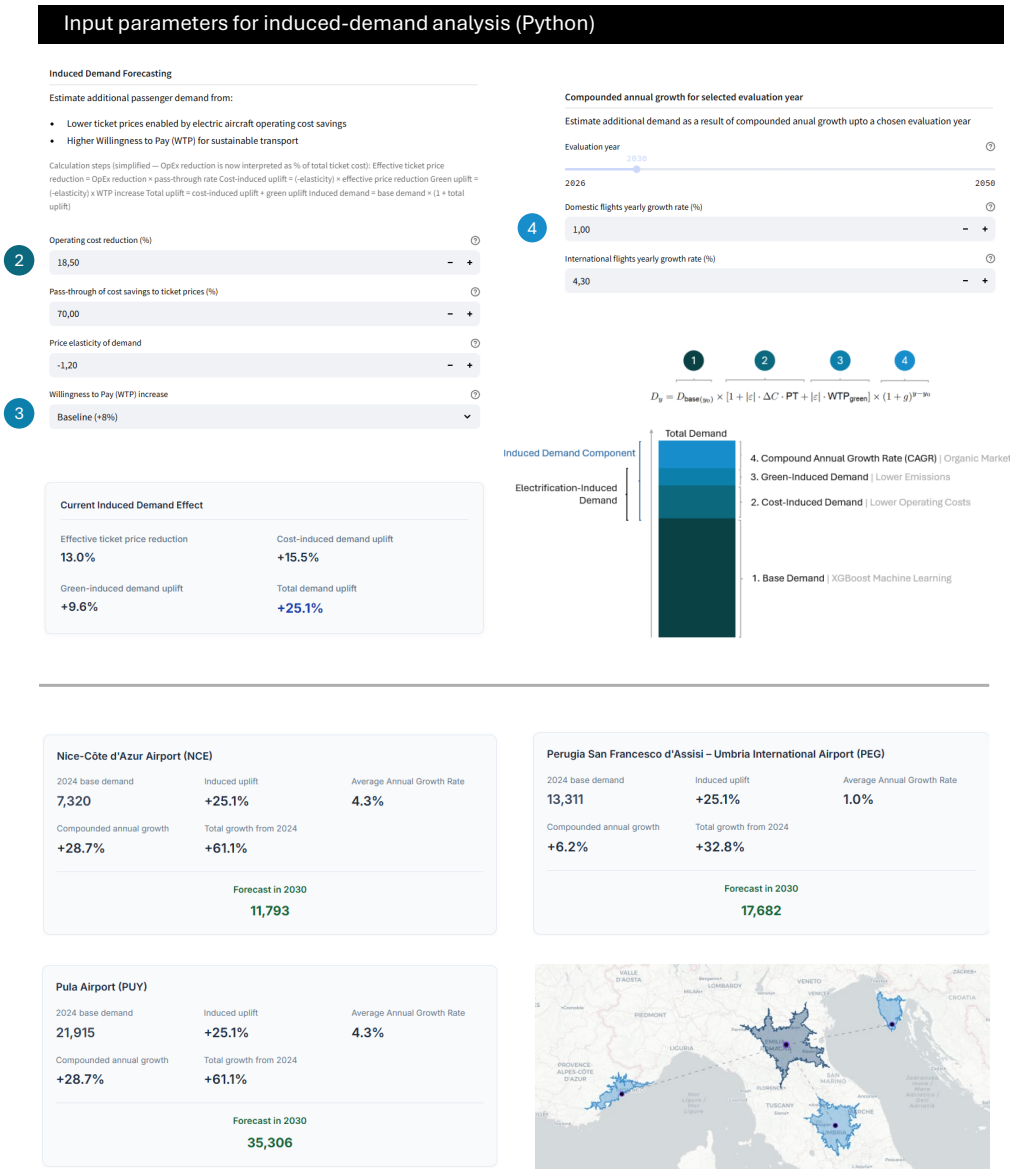

Figure 31: Input menu for the induced-demand analysis

F Integration with the 2040 TEN-T High-Speed Rail Network

Figure 32: Core HSR network of the TEN-T 2040 plan, as defined by the EU [10]

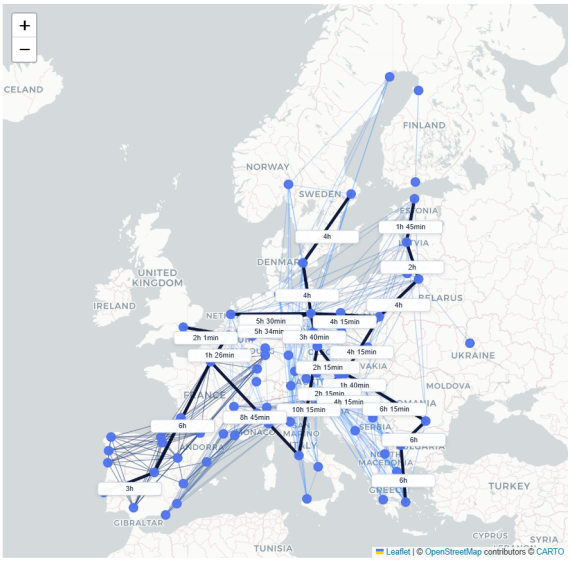

Figure 33: Programming of the core network [10], extended with additional data [12], leading to the full 2040 EU HSR network

G Daily Energy Demand Assessment at Proposed Hub Airports

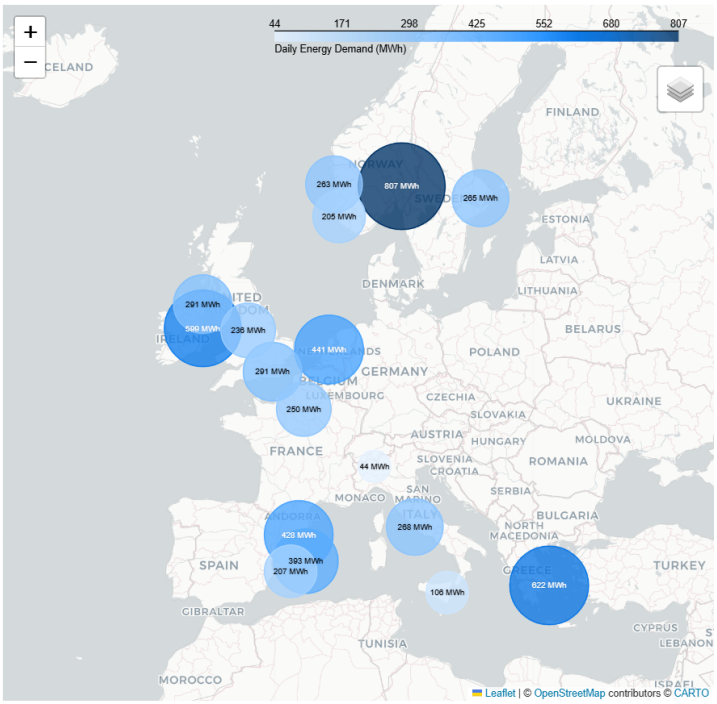

Figure 34: Energy demand of the identified hubs and connector airports for the proposed network of module 2.

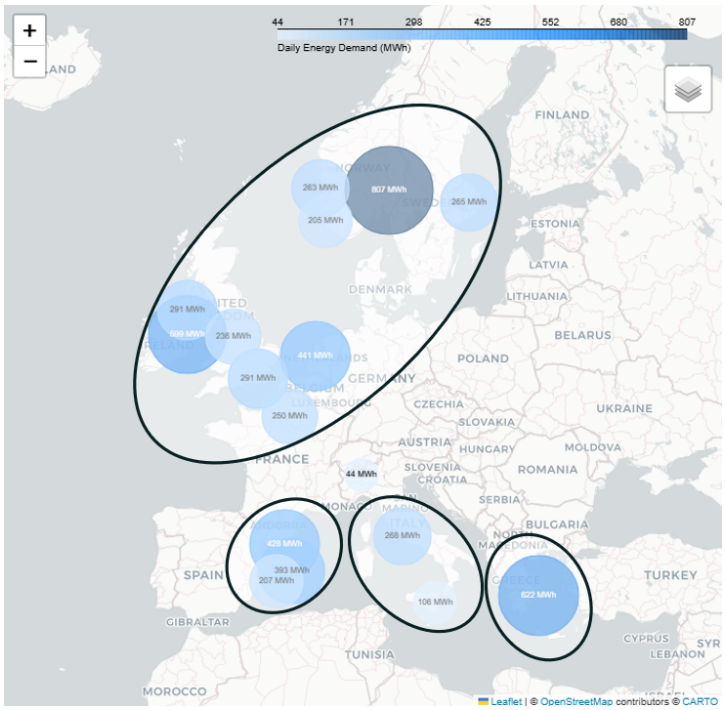

Figure 35: Energy demand within the clusters identified and visualised in Appendix D

H Network Configurations a Variety of Input Parameters

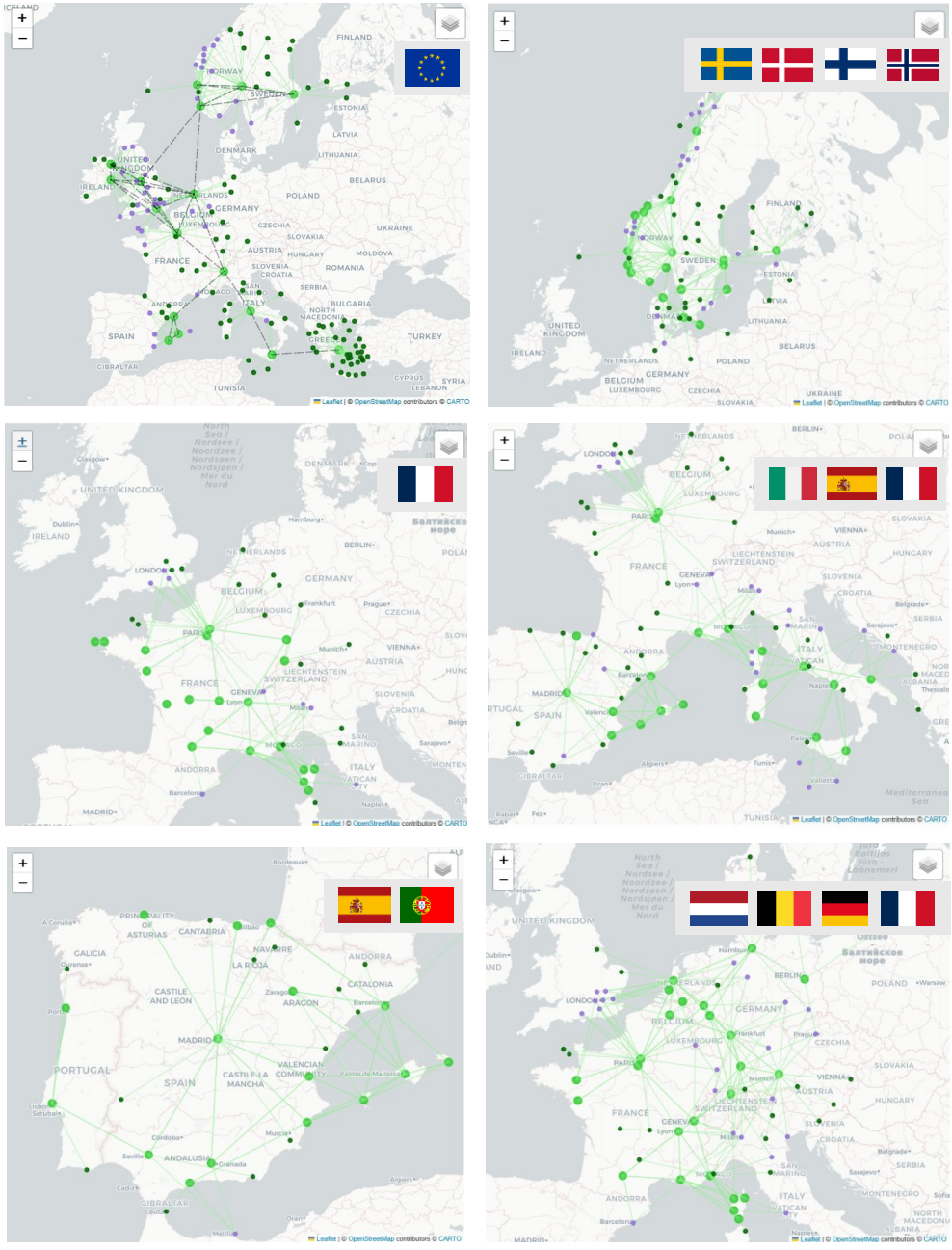

Figure 36: Output networks resulting from a variety of combinations of electric aircraft, countries and selected number of hubs with charging infrastructure

I Supplementary Network Extension Tools: Fleet Replacement, Route Feasibility, and Onward Connectivity Analysis

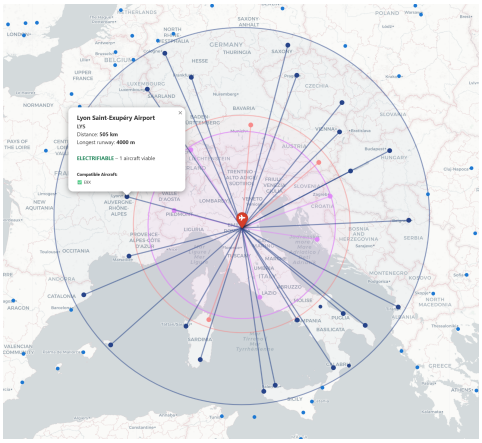

(a) Identification of electrifiable served routes

(b) Recommendation of electric aircraft type

Figure 37: Preliminary electrification analysis of served routes

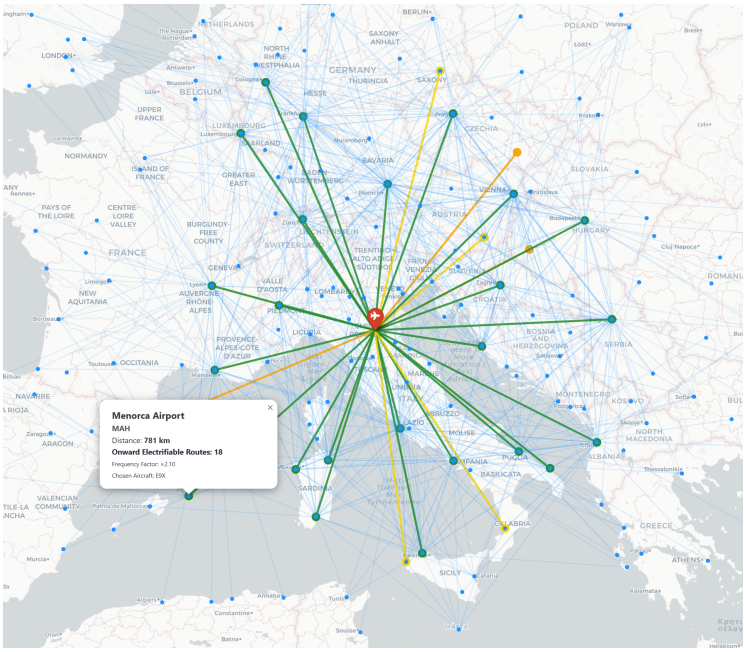

Figure 38: Assessment of onward electrifiable connections, departing from the destination airports

J Risk & Opportunity Analysis

Table 8: **Risks Associated with Battery-Electric Fixed-Wing Aircraft**

Category	Identifier	Risk Description
Technical	R-TEC-01	Insufficient gravimetric energy density of current battery technologies limiting practical range [15, 21, 60, 74]
	R-TEC-02	Battery degradation over charge/discharge cycles [26, 71]
	R-TEC-03	Limitations and penalties from high charge/discharge C-rates [21, 26]
Safety	R-SAF-01	Loss of all propulsion due to single-point battery or power distribution failure [32, 79]
	R-SAF-02	Crashworthiness and post-crash fire risks associated with integrated battery packs [54]
	R-SAF-03	Thermal runaway and thermal propagation in battery packs [54, 71, 74]
	R-SAF-04	High-voltage DC system hazards [32, 74]
Operational	R-OPS-01	Extended ground charging times limiting aircraft utilization and turnaround efficiency [21, 53, 74]
	R-OPS-02	Performance degradation in cold weather conditions [21, 74]
	R-OPS-03	Grid instability and capacity constraints from high-power charging demands [32, 53, 74]
	R-OPS-04	Increased flight frequency and airport capacity strain due to lower per-aircraft passenger capacity [60]
Certification	R-CER-01	Lengthy and complex certification processes due to evolving and immature regulatory frameworks [21, 42]
Economic	R-ECO-01	High upfront capital expenditure (CapEx) requirements [21, 44, 53]
	R-ECO-02	Supply-chain volatility for battery materials leading to price/availability shocks [71]
	R-ECO-03	Limited market adoption due to range and infrastructure constraints [21, 44, 60]
	R-ECO-04	Higher fleet acquisition and ownership costs due to the need for more aircraft to deliver equivalent passenger throughput [44, 60]
	R-ECO-05	Elevated crew and personnel costs from operating a larger fleet and higher flight frequency [21, 44]
Environmental	R-ENV-01	High environmental footprint from mining rare earth elements required for battery production [71]
	R-ENV-02	High energy intensity and carbon footprint of battery production and manufacturing [71, 92]
	R-ENV-03	Limited recycling rates and challenges with end-of-life battery disposal [86]
	R-ENV-04	Strong dependency on electricity grid decarbonisation for meaningful lifecycle emissions reductions [53, 92]

Table 9: **Opportunities Associated with Battery-Electric Fixed-Wing Aircraft**

Category	Identifier	Opportunity Description
Technical	O-TEC-01	Advanced power electronics for improved system efficiency [21, 85]
	O-TEC-02	Lightweight and compact airframe designs using advanced composites and topology optimisation to offset the heavy mass penalty of battery packs [87]
	O-TEC-03	Improved thermal management systems [21, 85]
	O-TEC-04	Distributed electric propulsion (DEP) [21, 49, 85]
Safety	O-SAF-01	Higher system reliability and lower mechanical failure rates due to the simplicity of electric motors [21]
	O-SAF-02	Enhanced monitoring and control of critical systems [85]
Operational	O-OPS-01	Reduced maintenance needs [21, 85]
	O-OPS-02	Lower noise propulsion systems [21]
Certification	O-CER-01	Increasing regulatory support and harmonization efforts for electric propulsion National Aviation Authorities Network [62]
Economic	O-ECO-01	Lower operating costs [21, 84, 85]
	O-ECO-02	New market segments in regional commercial aviation [7, 21, 40, 84, 85]
Environmental	O-ENV-01	Zero carbon emissions during flight [21, 59, 85]
	O-ENV-02	Complete elimination of in-flight non-CO_2 effects [21, 59, 72, 85]
	O-ENV-03	High energy efficiency of electric propulsion [21, 59, 85, 90]

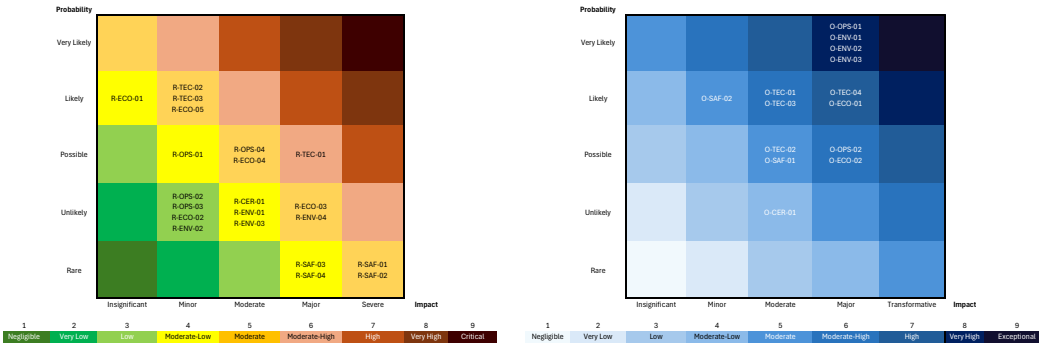

Figure 39: Risk & Opportunity matrices after secondary analysis